Global anthropogenic CO_2 emissions and uncertainties as prior for Earth system modelling and data assimilation

Margarita Choulga[1], Greet Janssens-Maenhout[2], Ingrid Super[3], Efisio Solazzo[2], Anna Agusti-Panareda[1], Gianpaolo Balsamo[1], Nicolas Bousserez[1], Monica Crippa[2], Hugo Denier van der Gon[3], Richard Engelen[1], Diego Guizzardi[2], Jeroen Kuenen[3], Joe McNorton[1], Gabriel Oreggioni[2], and Antoon Visschedijk[3]

[1]Research Department, ECMWF, Reading, RG2 9AX, United Kingdom
[2]European Commission, Joint Research Centre, JRC, Ispra, 21027, Italy
[3]TNO, Department of Climate, Air and Sustainability, Utrecht, 3584 CB, The Netherlands

Correspondence to: Margarita Choulga (margarita.choulga@ecmwf.int)

Abstract. The growth in anthropogenic carbon dioxide (CO_2) emissions acts as a major climate-change driver, which has widespread implications across society, influencing the scientific, political and public sectors. For an increased understanding of the CO_2 emission sources, patterns and trends, a link between the emission inventories and observed CO_2 concentrations is best established via Earth system modelling and data assimilation. Bringing together the different pieces of the puzzle of a very different nature (measurements, reported statistics and models) it is of utmost importance to know their level of confidence and boundaries well.

Inversions disaggregate the variation in observed atmospheric CO_2 concentration to variability in CO_2 emissions by constraining the regional distribution of CO_2 fluxes, derived either bottom-up from statistics or top-down from observations. The level of confidence and boundaries for each of these CO_2 fluxes is as important as their intensity, though often not available for bottom-up anthropogenic CO_2 emissions. This study provides a postprocessing tool CHE_UNC_APP for anthropogenic CO_2 emissions, to help assessing and managing the uncertainty of the different emitting sectors. The postprocessor is available under [https://doi.org/10.5281/zenodo.5196190]. Recommendations are given for regrouping the sectoral emissions, taking into account their uncertainty instead of their statistical origin, for addressing local hot spots, for the treatment of sectors with small budget but uncertainties larger than 100 %, and for the assumptions around the classification of countries based on the quality of their statistical infrastructure. This tool has been applied on the EDGARv4.3.2_FT2015 dataset, resulting in 7 input grid-maps with upper and lower uncertainty range for the European Centre for Medium-Range Weather Forecasts Integrated Forecasting System. The dataset is available under [https://doi.org/10.5281/zenodo.3967439]. While the uncertainty of most emission groups remains relatively small (5-20 %), the largest contribution (usually over 40 %) to the total uncertainty is determined by the OTHER group (of fuel exploitation and transformation but also agricultural soils and solvents) at global scale. The uncertainties have been compared for selected countries to those reported in the inventories submitted to the United Nations Framework Convention on Climate Change and to those assessed for the European emission grid-maps of the Netherlands Organisation for Applied Scientific

Research. Several sensitivity experiments are performed to check: 1) the country dependence – by analysing the impact of assuming either a well- or less well-developed statistical infrastructure, 2) the fuel type dependence – by adding explicit information for each fuel type used per activity from the Intergovernmental Panel on Climate Change, and 3) the spatial source distribution dependence – by aggregating all emission sources and comparing the effect against an even redistribution over the country. The first experiment shows the SETTLEMENT group (of energy for buildings) uncertainty changes the most when development level is changed. The second experiment shows that fuel specific information reduces uncertainty in emissions only when a country uses several different fuels in the same amount, when a country mainly uses globally most typical fuel for an activity uncertainty values computed with and without detailed fuel information are the same. The third experiment highlights the importance of spatial mapping.

1 Introduction

Accurate assessment of anthropogenic carbon dioxide (CO_2) emissions is important to better understand the global carbon cycle. Efforts towards a global anthropogenic CO_2 monitoring and verification support capacity as described by Janssens-Maenhout et al. (2020), rely on atmospheric modelling and atmospheric observations (in-situ from, for example, the Integrated Carbon Observation System, ICOS, air-borne e.g. aircraft campaigns, or space-borne e.g. the Orbiting Carbon Observatory, OCO-2, and the Greenhouse gases Observing Satellite, GOSAT). Atmospheric measurements of CO_2 and co-emitted species can be assimilated into flux inversion systems to provide top-down estimates of CO_2 fluxes at multiple spatiotemporal scales. The European Centre for Medium-Range Weather Forecasts (ECMWF), for example, aims to develop an operational inversion system to estimate CO_2 fluxes using observed atmospheric concentrations of CO_2 and other relevant species.

The global transport models require an initial best estimate of the CO_2 emission fields with uncertainties, the so-called "prior information". The intensity of the emission fields is corrected through minimization of the difference between the modelled and measured concentration values for CO_2. The uncertainty of these corrected CO_2 fluxes based on inverse modelling will be lower with the increase of CO_2 observations and its accuracy. The disentanglement of the fossil CO_2 emissions from the total atmospheric CO_2 emissions remains challenging. For example in 2018 total anthropogenic CO_2 concentrations (5.4 ± 0.4 ppm) represented only 1.3 % of the global atmospheric CO_2 concentration (407.4 ± 0.1 ppm) (Friedlingstein et al., 2019), which states the need for a high accuracy of measurements (≥ 1.0 %).

Emission fields are often supplied through emission inventories. Bottom-up emission inventories start from human activity statistics. Emission factors are defined for each activity and provided at international or country level (e.g. National greenhouse gas Inventory Report, NIR). Such inventories need to be gridded and characterised with uncertainties to represent a prior data set useful for numerical modelling. Table 1 shows examples of most commonly used global gridded CO_2 emission datasets, for more details see Cong et al. (2018, Table 1), Janssens-Maenhout et al. (2019, Table 3), Andrew (2020), and Jones et al. (2021).

Table 1: Examples of global gridded anthropogenic CO_2 emission bottom-up datasets

Name	Resolution	Period	Main assumptions, uncertainties	Source
Carbon Dioxide Information Analysis Center (CDIAC)	Spatial: 1.0º×1.0º Temporal: annual, monthly Sectoral: 1	1751-2013	Use population density to disaggregate emissions, the mass-emissions data based on fossil-fuel consumption estimates. Provide gridded annual and monthly uncertainty estimates for 1950-2013.	Andres et al., 1996; Andres et al., 2016
Open-Data Inventory for Anthropogenic Carbon dioxide (ODIAC)	Spatial: 1×1 km^2, 0.1º×0.1º Temporal: monthly Sectoral: 6	1979-2018	First introduced the combined use of nightlight data and individual power plant emission/ location profiles.	Oda and Maksyutov, 2011; Oda et al. 2018; ODIAC, 2020
Emissions Database for Global Atmospheric Research (EDGAR)	Spatial: 0.1º×0.1º Temporal: annual, monthly Sectoral: 26	1970-(year-1)	Based on international statistics, covers all IPCC (2006) reporting categories, consistent methodology applied to all the world countries.	Janssens-Maenhout et al., 2019
Fossil Fuel Data Assimilation System (FFDAS)	Spatial: 0.1º×0.1º Temporal: annual Sectoral: 2	1997-2012	Provide gridded posterior uncertainty (version 2.2); in addition, provide monthly, weekly, and hourly fractions from annual CO_2 emissions.	Asefi-Najafabady et al., 2014
Community Emissions Data System (CEDS)	Spatial: 0.1º×0.1º Temporal: annual, monthly Sectoral: 55	1750-2014	Provide emissions of CO_2 and other GHGs and pollutants.	Hoesly et al., 2018
Peking University Fuel combustion inventory (PKU-FUEL)	Spatial: 0.1º×0.1º Temporal: monthly Sectoral: 6	1960-2014	By request provide daily emissions and the results of Monte Carlo simulation-based uncertainty analyses.	Chen et al., 2016; Liu et al., 2015
Global Carbon Budget Gridded Fossil Emissions Dataset (GCP-GridFED)	Spatial: 0.1º×0.1º Temporal: monthly Sectoral: 28	1959-2018	National GHG inventories reported to UNFCCC are used for the GCP dataset, that is gridded with predefined grid-maps following EDGARv4.3.2 spatial distribution proxies; also provide gridded sectoral uncertainties	Jones et al., 2021

Only four datasets from Table 1 provide uncertainty estimates, namely CDIAC, FFDAS, PKU-FUEL and GCP-GridFED. CDIAC uncertainties have no sectors and include contributions from the tabular fossil fuel CO_2 emissions (assigned per 7 country types, values are constant over time), geography map (power plant location), and population map (has details both in time and space, and used to distribute fossil fuel CO_2 emissions). Population map uncertainty strongly dominates in the generated gridded fossil fuel CO_2 uncertainties (Andres et al., 2016). CDIAC uncertainties have no sectoral distribution and are presented on 1.0º×1.0º grid. FFDAS provides only posterior uncertainties, which are based on a model inversion. These posterior uncertainties could be used as prior uncertainties for separate inversion systems. However, this would make the characterisation of uncertainty more complex if there were similarities in the model and observations used. PKU-FUEL uncertainty estimates of CO_2 emission maps, associated with uncertain fuel data and uncertain activity data in the spatial disaggregation process, are based on Monte Carlo ensemble simulations. Input data was randomly sampled 1000 times from an a priori normal uncertainty distribution with a certain coefficient of variation: for fuel consumptions from ships/aviation, the sector coefficient of variation is set to be 20 %, for the wildfires sector 18 %, for all other fuel data 10 %, for combustion rates 20 % (Marland et al., 2003; Marland et al., 2006; Wang et al., 2013; Oda et al, 2019). GCP-GridFED focusses strongly

on the fuel disaggregation for the global CO_2 emissions, for which a detailed assessment of the uncertainty has not yet been published.

2 Methods

2.1 Purpose and UNFCCC context

Intercomparisons of global greenhouse gas (GHG) emission inventories were carried out (e.g. Cong et al., 2019; Petrescu et al., 2020) to better understand discrepancies and missing or lesser-known sources. The United Nations Framework Convention on Climate Change (UNFCCC) experts, reviewing national GHG inventories on a yearly basis, are keen to know which sectors or fuels need extra attention for an inventory that complies with the principles of transparency, accuracy, consistency, completeness and comparability (TACCC-principles). Discrepancies are often related to the different interpretations of definitions or to missing information (statistics and/or measurements). When focussing on global emission datasets, which are calculated bottom-up following the Intergovernmental Panel on Climate Change (IPCC) 2006 Guidelines for National Greenhouse Gas Inventories, then the discrepancy using different definitions disappears, while the lack of information becomes strongly apparent for certain regions. More information costs time and effort, when compiling a global dataset in a consistent way. Therefore, it is of paramount importance to prioritise the additional information needs and the weaknesses in the inventory with sources of large uncertainty in intensity or variability.

IPCC has been addressing uncertainty from the beginning. Methodology, data, and data sources in this paper were taken from IPCC (2006) guidelines and its refinements (IPCC, 2019). Also, the assumptions are based on IPCC (2006), so all emissions are considered to be fully uncorrelated by activity (and so by sector and by type) (i.e. all activities from IPCC (2006) are fully uncorrelated with each other), for the calculation of the uncertainty as well as of the covariance matrices.

While the UNFCCC sticks to national inventories, the atmospheric modelling community needs spatially distributed data. This adds an extra uncertainty to the emission grid-maps, not evaluated with the uncertainty of the proxy data but which needs an assessment of the representativeness of the selected proxies for distributing the emissions. The point sources, leading to large plumes, were prioritised for being treated separately with more data. These consisted of super power plants, which are defined as a large power plant or a group of closely located power plants (operating at maximum capacity and availability), causing CO_2 plumes from a single grid cell with a CO_2 flux $\geq 7.9 \cdot 10^{-6}$ $kg \cdot m^{-2} \cdot s^{-1}$. According to expert knowledge, the upper bound of annual uncertainty for super power plants is not larger than +3.0 %, whereas for small plants whose operation is decided on day-to-day needs, this can reach up to +15.0 %. In this paper, 30 grid-cells of 0.1º×0.1º from 12 countries were identified, representing these super power generators (896.7 Mt of the energy sector) and including large plants from China, Russia and India (for the detailed ranking of the power plant sites in function of their emission intensity, refer to the Supplementary Information, section S.1). The power plant coordinates were checked, to avoid the need for an uncertainty related to their positioning. The remaining power plants (not super power generators), over 30000, could not be checked to the same extent and therefore are recommended in a second emission group.

2.2 Generating uncertainty input for transport models

The uncertainty calculation methodology and initial uncertainty values (i.e. activity data and emission factor uncertainties per CO_2-emitting activity) are both taken from IPCC (2006) and its refinements (IPCC, 2019). The following terminology is used to ease the explanation: "activity" – IPCC (2006) activities which result in anthropogenic CO_2 emissions in the yearly budget (a long-cycle carbon); "sector" – combination of different activities that are measured/reported together (that have emission budget data); "group" – combination of different "sectors", that have emission budget data, purely for modelling/comparison needs.

In general, uncertainties are calculated in three steps: (i) "sector" uncertainties (based on emission factors and activity data uncertainties), (ii) annual grouped uncertainties, and (iii) monthly grouped uncertainties. By default, all calculations are performed separately for upper and lower half-ranges of uncertainties and "sector"/"group" combined uncertainties, where upper and lower uncertainty half-ranges are in percent.

2.2.1 Calculating "sector" uncertainties

The initial 92 IPCC (2006) activity uncertainties are combined into "sectors" for which the user has emission budget data[1], following Eq. (1) and Eq. (2):

$$UC_{activity\_i} = \sqrt{EF^2_{activity\_i} + AD^2_{activity\_i}}, \quad (1)$$

where combined uncertainties $UC_{activity\_i}$ per activity i were calculated using uncertainties for emission factors $EF_{activity\_i}$ and activity data $AD_{activity\_i}$ in percent provided in IPCC (2006) and its refinements (IPCC, 2019);

$$UC_{sector\_j} = \sqrt{UC^2_{activity\_1} + UC^2_{activity\_2} + \ldots + UC^2_{activity\_n}}, \quad (2)$$

where combined uncertainties UC_{sector_j} per "sector" j were calculated with the error propagation method, taking into account particular for that "sector" activity combined uncertainties $UC_{activity\_1}$, $UC_{activity\_2}$,..., $UC_{activity\_n}$ used in percent.

2.2.2 "Group" annual uncertainties

This concerns the further grouping of the combined IPCC (2006) "sectors" according to the user needs into "groups" and calculation of "group" yearly uncertainties. Usually, there are computational restrictions for operational modelling: the number of emission input fields read by the model can't be too large or emission values are too low to be distinguishable from a global or large regional modelling perspective, so some "sectors" need to be merged. In addition, instantaneous local emission data as an aggregated total might be rather uncertain and hard to evaluate for different emission types all over the world. IPCC (2006) and its refinement (IPCC, 2019) provide the best possible information on how certain emissions are reported on an annual national level.

[1] Often, emission budgets are provided not per IPCC (2006) activity but for several activities together (usually due to measuring/reporting limitations), for which the user then needs to assume a lump sum activity, emission factor and uncertainties of those.

"Sector" uncertainties have to be adjusted to consider a country's statistical system development level and its yearly emission budget, log-normal distribution of non-negative emissions, and then further combined into "group" uncertainties for modelling/comparison purposes in the following way (by default all calculations are performed separately for upper and lower half-ranges of uncertainties):

$$FC_{sector\_j} = \left[\frac{-0.7200+1.0921\cdot UC_{sector\_j}-1.63\cdot 10^{-3}\cdot UC_{sector\_j}^{2}+1.11\cdot 10^{-5}\cdot UC_{sector\_j}^{3}}{UC_{sector\_j}}\right]^{2}, \quad (3)$$

$$\left(UC_{sector\_j}\right)_{corr} = \begin{cases} UC_{sector\_j}\cdot FC_{sector\_j}, 100\% \le UC_{sector\_j} \le 230\% \\ UC_{sector\_j}, UC_{sector\_j} < 100\% \cup UC_{sector\_j} > 230\% \end{cases}, \quad (4)$$

where corrected uncertainties $(UC_{sector\_j})_{corr}$ per "sector" j were calculated to take into account large combined uncertainty (100 % ≤ UC_{sector_j} ≤ 230 %), underestimation by the error propagation method in comparison to a Monte Carlo simulation, correction factor FC_{sector_j} is computed based on Frey (2003), also log-normal adjustment of the emission distribution is computed based on Frey (2003) as detailed in the Supplementary Information, section S.3;

$$UC_{group\_k} = \frac{\sqrt{\left(\left\{\left(UC_{sector\_1}\right)_{corr}\right\}_{ln}\cdot E_{sector\_1}\right)^{2}+\left(\left\{\left(UC_{sector\_2}\right)_{corr}\right\}_{ln}\cdot E_{sector\_2}\right)^{2}+\cdots+\left(\left\{\left(UC_{sector\_n}\right)_{corr}\right\}_{ln}\cdot E_{sector\_n}\right)^{2}}}{\left|E_{sector\_1}+E_{sector\_2}+\cdots+E_{sector\_n}\right|}, \quad (5)$$

$$E_{group\_k} = E_{sector\_1} + E_{sector\_2} + \cdots + E_{sector\_n}, \quad (6)$$

where the combined uncertainties UC_{group_k} and total emissions E_{group_k} per "group" k were calculated taking into account specifically for that "group" "sector" log-normally transformed uncertainties $\left\{\left(UC_{sector\_1}\right)_{corr}\right\}_{ln}, \left\{\left(UC_{sector\_2}\right)_{corr}\right\}_{ln}, \ldots, \left\{\left(UC_{sector\_n}\right)_{corr}\right\}_{ln}$ in percent.

"Group" upper and lower uncertainty half-range values are descriptive, but not straightforward to use in numerical modelling (e.g. emission perturbations in ensemble runs, flux inversions), so mean μ^{ln} and standard σ^{ln} deviation of the "group" log-normal distribution are calculated starting from Eq. (7):

$$E_{group\_k} = e^{\mu^{ln}+\sigma^{ln}\cdot z}, \quad (7)$$

where z is a standard normal variable, and parameters μ^{ln} and σ^{ln} represent a natural logarithm of "group" emissions, not the emissions themselves. The lower and upper bounds of the 95 % probability range, which are the 2.5th and 97.5th percentiles respectively, are calculated assuming a log-normal distribution based on a corrected estimated uncertainty half-range from the error propagation approach, and are lower and upper uncertainty values. Taking this into account and using the Z-table for 2.5th and 97.5th percentiles p ($p_{2.5} = -1.96, p_{97.5} = 1.96$), mean μ^{ln} and standard deviation σ^{ln} of log-normal distribution can be calculated following Eq. (8):

$$Z_p = \frac{ln\left(\left[E_{group\_k}\right]_p\right)-\mu_{group\_k}^{ln}}{\sigma_{group\_k}^{ln}}, \quad (8)$$

resulting in Eq. (9) and Eq. (10):

$$\mu_{group\_k}^{ln} = ln\left(E_{group\_k}\right) + \frac{1}{2} ln\left(1 + \frac{\left[UC_{group\_k}\right]_{low}}{100\%}\right) + \frac{1}{2} ln\left(1 + \frac{\left[UC_{group\_k}\right]_{high}}{100\%}\right), \quad (9)$$

$$\sigma_{group\_k}^{ln} = \frac{ln\left(1+\frac{\left[UC_{group\_k}\right]_{low}}{100\%}\right) - ln\left(1+\frac{\left[UC_{group\_k}\right]_{high}}{100\%}\right)}{-3.92}, \quad (10)$$

where $\left[UC_{group\_k}\right]_{low}$ and $\left[UC_{group\_k}\right]_{high}$ are in percent.

Figure 1 shows a simplified roadmap for yearly uncertainty calculations.

	GROUP 1						…	GROUP k		…	…	GROUP C	
	SECTOR 1				SECTOR 2			SECTOR j				SECTOR B	
	ACTIVITY 1		ACTIVITY 2		ACTIVITY 3		…	ACTIVITY i		…	…	ACTIVITY A	
Uncertainty per ACTIVITY	Emission Factor$_1$	Activity Data$_1$	Emission Factor$_2$	Activity Data$_2$	Emission Factor$_3$	Activity Data$_3$	…	Emission Factor$_i$	Activity Data$_i$	…	…	Emission Factor$_A$	Activity Data$_A$
	Combined$_1$		Combined$_2$		Combined$_3$		…	Combined$_i$		…	…	Combined$_A$	
Uncertainty per SECTOR	Combined$_1$				Combined$_2$			Combined$_j$				Combined$_B$	
	Corrected for large values$_1$				Corrected for large values$_2$			Corrected for large values$_j$				Corrected for large values$_B$	
	Log-normal transformation$_1$				Log-normal transformation$_2$			Log-normal transformation$_j$				Log-normal transformation$_B$	
Uncertainty per GROUP	Combined$_1$							Combined$_k$				Combined$_C$	
	Parameters of log-normal distribution$_1$							Parameters of log-normal distribution$_k$				Parameters of log-normal distribution$_C$	

Figure 1: Yearly uncertainty calculation simplified roadmap.

2.2.3 "Group" monthly uncertainties

The "group" monthly uncertainties are calculated starting from the yearly uncertainties, which can provide a more appropriate variation than the yearly timescale for operational modelling. In this way, yearly "sector" uncertainties are adjusted to represent monthly variability (no correlation between months is assumed), and further combined into "group" monthly uncertainties, by means of the following four steps:

1) the same steps as for annual uncertainty calculation are used but based on monthly emission budgets (i.e. uncertainties for IPCC activities are combined to "sectors" with the error propagation method, corrected for systematic underestimation by the error propagation method, and adapted to have log-normal distribution);

2) the correlation α (an uncertainty boosting parameter) between yearly and monthly uncertainties is based on an analysis of the variations over the different months following Eq. (11). It's computed to enhance obtained monthly

uncertainties as they are the same or even smaller than the yearly ones, because empirical equations applied use emission budgets, which are smaller for individual months compared to the yearly values:

$$(E_{YEAR} \cdot UC_{YEAR})^2 = \alpha^2 \cdot ((E_{MONTH1} \cdot UC_{MONTH1})^2 + (E_{MONTH2} \cdot UC_{MONTH2})^2 + \cdots + (E_{MONTH12} \cdot UC_{MONTH12})^2), \quad (11)$$

where E and UC correspond to "sector" emission budget and uncertainty in kilotonne and % respectively, *YEAR,MONTH1,MONTH2,…,MONTH12* – yearly and monthly (January, February, …, December) values. Eq. (11) is based on the rule for combining uncorrelated uncertainties under addition of the error propagation equation (see Eq. (5)) and the assumption that each month's uncertainty should be enhanced (boosted) by the same value;

3) the prior yearly "sector" uncertainties are multiplied by the boosting parameter (specific per country and emission "sector") and the results are used as a first guess of prior month "sector" uncertainties;

4) the calculation steps 1) to 3) are iterated to find the best boosting parameter as the best fit between yearly and combined 12-month uncertainties, with the incremental step below a given acceptable threshold from Eq. (11) for each country and emission "sector". With this optimum boosting parameter, monthly uncertainties per "sector" are calculated and then merged into "groups", with a log-normal distribution of CO_2 emissions.

Detailed information on each Unix shell script included in the anthropogenic CO_2 emission uncertainty calculation tool CHE_UNC_APP (Choulga et al., 2021) is provided in the Supplementary Information, section S.4.

2.2.4 Remarks about the fuel dependence and assumptions concerning correlation

It should be noted that IPCC (2006) provide default emission factor values for different fuels in transport-related activities (e.g. railways, aviation, etc.). Detailed fuel consumption information per IPCC activity, that result in a long-cycle carbon, was not available and instead the most typical and consumed (common) fuel type (or its emission factor value) was used:

- Aviation cruise (1.A.3.a_CRS), climbing & descent (1.A.3.a_CDS), and landing & take off (1.A.3.a_LTO) – jet kerosene;
- Road transportation (1.A.3.b), and pipelines, off-road transport (1.A.3.e) – most typical emission factor uncertainty;
- Shipping (1.A.3.d) – composition of 80 % diesel and 20 % residual fuel oil;
- Railways (1.A.3.c) – diesel.

It should also be noted that some uncertainty ranges for emission factors and/or activity data in IPCC (2006) and its refinements (IPCC, 2019) are not symmetrical and have higher uncertainty values for the lower bound than for the upper bound (or vice versa), due to input from expert knowledge or available in-situ data, which then leads to the same pattern in final prior uncertainty bounds.

It should finally be noted that according to the IPCC (2006), all anthropogenic CO_2 emissions are assumed to be fully uncorrelated, hence the prior error correlations between grid-cell emissions from the same "sector"/"group" should be assumed negligible if country- and/or sector-specific information is lacking.

3 Uncertainty calculation application

The method explained above has been applied to the EDGARv4.3.2_FT2015 dataset to prepare prior uncertainty information for the ECMWF Integrated Forecasting System (IFS) model.

3.1 Data input

In this example, 2015, the year of the Paris Agreement and reference for several Nationally Determined Contributions, is chosen as a base year to analyse anthropogenic CO_2 budgets (i.e. global, regional, national) from different sources (i.e. global statistics, national reports), benefitting the availability of observations (both in-situ ground and space-borne) as well as reported and verified emission inventories.

Following IPCC (2006) and its refinements (IPCC, 2019), starting from the global fossil CO_2 grid-maps of EDGAR inventory versions 4.3.2 (Janssens-Maenhout et al., 2019) and 4.3.2_FT2015 (Olivier et al., 2016a), for 2012 and 2015 respectively, an updated emission dataset CHE_EDGAR-ECMWF_2015 [2] (Choulga et al., 2020) is derived. The EDGARv4.3.2 dataset is improved by correcting the allocation of the autoproducers to the manufacturing sector instead of the energy sector. Autoproducers are defined by International Energy Agency (IEA) and include the energy (electricity and heat) generated by an industry for its own use, mostly for the manufacturing. An extra emission source of fugitive CO_2 from coal mines is also added, following the recommendations from IPCC (2019). Even though this emission source is not that large globally, usually the coalseam gas is composed dominantly of methane (CH_4), but in some coalmines (in Australia, and also in Brazil) seam gas consists predominantly (> 95 %) of CO_2 (Beamish and Vance, 1992), leading to significant atmospheric CO_2 concentration increases. An additional map for CHE_EDGAR-ECMWF_2015 with coal mining emissions from underground mines has been generated, following the IPCC (2019) default values and the coal mining activity of CH_4 emission grid-maps from hard and brown coal production in EDGARv4.3.2 (for more information refer to the Supplementary Information, section S.2). For the update from 2012 to 2015 the fast-track approach of Olivier et al. (2016b) is used. The initial 92 IPCC activity uncertainties are combined into 20 EDGAR "sectors" for two distinct country types with well- and less well-developed statistical infrastructures (i.e. country's ability to register different emissions – tabulate even very small emissions or only major ones, respectively). For the input to the IFS model the emission "sectors" are grouped in 7 "groups", with one "group" devoted to super power plants. Table 2 shows activity and "sector" grouping and emission budget difference between EDGARv4.3.2_FT2015 and CHE_EDGAR-ECMWF_2015 datasets due to reallocation of the autoproducers from the energy sector (-8 %) to the manufacturing sector (+18 %), and due to the extra emission source of diffusive coal mine CO_2.

Table 2: Grouping of anthropogenic long-cycle carbon CO_2 emission "sectors" into "groups", note provides main information and typical fuel type, global emission budgets for 2015 in megatonne provides values for EDGARv4.3.2_FT2015 (total sum 35986.5 Mt)

[2] CHE stands for the CO_2 Human Emissions project (CHE, 2020).

and CHE_EDGAR-ECMWF_2015 (total sum 35995.2); *italics* – values with biggest differences, * – values that were replaced from EDGARv4.3.2

№	"Group" name	IPCC (2006) activities per "sector"	Note	Emission budget 2015, Mt			
				EDGARv4.3.2_FT2015		CHE_EDGAR-ECMWF_2015	
1	ENERGY_S	1.A.1.a (subset)	Power industry (without autoproducers): super emitting power plants	*13704.0*	*13841.2*	*896.7*	*12705.5*
2	ENERGY_A	1.A.1.a (rest)	Power industry (without autoproducers): standard emitting power plants			*11671.6*	
		4.C	Solid waste incineration	137.2		137.2	
3	MANUFACTURING	1.A.2	Combustion for manufacturing (including autoproducers)	*6182.8*	*8960.1*	*7320.4*	*10096.0*
		2.C.1, 2.C.2	Iron and steel production	233.6		233.6	
		2.C.3, 2.C.4, 2.C.5, 2.C.6, 2.C.7	Non-ferrous metals production	91.4		91.4	
		2.D.1, 2.D.2, 2.D.4	Non energy use of fuels	24.7*		24.6	
		2.A.1, 2.A.2, 2.A.3, 2.A.4	Non-metallic minerals production	1748.8		1749.0	
		2.B.1, 2.B.2, 2.B.3, 2.B.4, 2.B.5, 2.B.6, 2.B.8	Chemical processes	678.8*		677.0	
4	SETTLEMENTS	1.A.4, 1.A.5.a, 1.A.5.b.i, 1.A.5.b.ii	Energy for buildings	3321.9	3321.9	3322.7	3322.7
5	AVIATION	1.A.3.a_CRS	Aviation cruise; typical fuel: jet kerosene	412.2	815.4	412.2	815.4
		1.A.3.a_CDS	Aviation climbing & descent; typical fuel: jet kerosene	305.5		305.5	
		1.A.3.a_LTO	Aviation landing & take off; typical fuel: jet kerosene	97.7		97.7	
6	TRANSPORT	1.A.3.b	Road transportation; typical fuel: most typical emission factor uncertainty	5530.2	6604.4	5530.6	6604.9
		1.A.3.d	Shipping; typical fuel: composition of 80 % diesel and 20 % residual fuel oil	819.0		819.1	
		1.A.3.c, 1.A.3.e	Railways, pipelines, off-road transport; typical fuel: railways – diesel, off-road transport – most typical emission factor uncertainty	255.2		255.2	
7	OTHER	1.A.1.b, 1.A.1.c, 1.A.5.b.iii, 1.B.1.c, 1.B.2.a.iii.4, 1.B.2.a.iii.6, 1.B.2.b.iii.3	Oil refineries and transformation industry	1917.4	2443.5	1917.8	2450.6
		1.B.2.a.ii, 1.B.2.a.iii.2, 1.B.2.a.iii.3, 1.B.2.b.ii, 1.B.2.b.iii.2, 1.B.2.b.iii.4, 1.B.2.b.iii.5, 1.C	Fuel exploitation	258.4		258.4	
		1.B.1.a	Coal production	*0.0*		*7.0*	
		3.C.2, 3.C.3, 3.C.4, 3.C.7	Agricultural soils	99.0		99.1	
		2.D.3, 2.B.9, 2.E, 2.F, 2.G	Solvents and products use	168.7*		168.3	

3.2 Model constraints

The operational IFS model is used to provide global CO_2 forecasts using the gridded prior emissions previously described (Agusti-Panareda et al., 2014; Agusti-Panareda et al., 2019). A prototype 4D-Var inverse modelling system is currently under development to monitor anthropogenic CO_2 emission using the IFS. There is also an on-going development to extend the window length beyond 24-hours using an ensemble-based methodology.

The uncertainties derived for the 7 "groups" described here have been used to generate an ensemble of forecasts for 2015 based on the operational IFS ensemble system (McNorton et al., 2020). This provides a representation of the model uncertainty and an estimation of the expected signal-to-noise ratio for a future inverse modelling system. Random seeds for each "group" and country were applied to the normalised log-normal mean μ^{ln} and standard deviation σ^{ln} to generate emission scaling factors, which were then used for 50 ensemble members.

Primarily, the derived emission uncertainties presented here are envisaged for use as prior errors within atmospheric inversion frameworks. Aggregation of emission "sectors" into 7 "groups" is required for computational efficiency and to reduce the dimensions of the inverse problem. To resolve collocated emissions, further information is required about spatial correlations and/or co-emitted species (e.g. nitrogen oxides (NO_x)). Within the IFS inversion prototype, the log-normal normalised standard deviation outlined in the previous section is used to provide the uncertainty values to prevent negative scaling factors.

3.3 CHE_EDGAR-ECMWF_2015 output

The new CHE_EDGAR-ECMWF_2015 dataset with anthropogenic fossil CO_2 emissions and their uncertainties was compiled and tested at ECMWF. The fossil CO_2 emissions include all long-cycle carbon emissions from human activities, such as fossil fuel combustion, industrial processes (e.g. cement) and products use, but excludes emissions from land-use change and forestry. Human CO_2 emission inventories were processed into gridded $0.1^o \times 0.1^o$ resolution maps to provide an estimate of prior CO_2 emissions, aggregated in 7 main emissions "groups": 1) energy production by super-emitters, 2) energy production by standard-emitters, 3) manufacturing, 4) settlements, 5) aviation, 6) other transport at ground level and 7) others, with an estimation of their uncertainty and covariance. Aggregation of the IPCC activities and "sectors" into "groups" was based on similarities between the magnitude of uncertainty, the spatiotemporal correlation and co-emission factors of each "sector". It is assumed that each emission "group" is fully correlated with itself and fully uncorrelated with any other "group" (only diagonal values of the 7×7 "groups" covariance matrix for the atmospheric transport model are non-zero and equal to log-normal variance). The CHE_EDGAR-ECMWF_2015 data are freely available [https://doi.org/10.5281/zenodo.3967439], and consist of 11 grid-maps in NetCDF format and one Excel file with information on anthropogenic CO_2 emissions and their uncertainties. For detailed information on each file see Table 3.

Table 3: Detailed information on CHE_EDGAR-ECMWF_2015 data

File	General note	Field / Spreadsheet
Annual_Upper_Lower_Uncertainties_Percentage_0.1_0.1.nc	file has 2×8 fields with annual upper and lower uncertainty bounds in percent per emission "group" and for all "groups" summed together on a regular grid with 1800 pixels along the latitude and 3600 pixels along the longitude, where values represent centre of the grid-cell	"Lower" – lower uncertainty bound (2.5th percentile of log-normal distribution) for yearly emissions, in percent
		"Upper" – upper uncertainty bound (97.5th percentile of log-normal distribution) for yearly emissions, in percent
		"Sector" – emission "sector" numerical name. "0" represents emission "group" ENERGY_S (with IPCC (2006) activity 1.A.1.a (subset)) standing for power industry emissions from super emitting power plants; "1" ENERGY_A (1.A.1.a (rest), 4.C) – power industry emissions from standard emitting power plants, & solid waste incineration; "2" MANUFACTURING (1.A.2, 2.C.1, 2.C.2, 2.C.3, 2.C.4, 2.C.5, 2.C.6, 2.C.7, 2.D.1, 2.D.2, 2.D.4, 2.A.1, 2.A.2, 2.A.3, 2.A.4, 2.B.1, 2.B.2, 2.B.3, 2.B.4, 2.B.5, 2.B.6, 2.B.8) – combustion for manufacturing (including autoproducers), & iron and steel production, & non-ferrous metals production, & non energy use of fuels, & non-metallic minerals production, & chemical processes; "3" SETTLEMENTS (1.A.4, 1.A.5.a, 1.A.5.b.i, 1.A.5.b.ii) – energy for buildings, residential heating; "4" AVIATION (1.A.3.a_CRS, 1.A.3.a_CDS, 1.A.3.a_LTO) – aviation cruise, & climbing and descent, & landing and take off; "5" TRANSPORT (1.A.3.b, 1.A.3.d, 1.A.3.c, 1.A.3.e) – road transportation, & shipping, & railways, pipelines, off-road transport; "6" OTHER (1.A.1.b, 1.A.1.c, 1.A.5.b.iii, 1.B.1.c, 1.B.2.a.iii.4, 1.B.2.a.iii.6, 1.B.2.b.iii.3, 1.B.2.a.ii, 1.B.2.a.iii.2, 1.B.2.a.iii.3, 1.B.2.b.ii, 1.B.2.b.iii.2, 1.B.2.b.iii.4, 1.B.2.b.iii.5, 1.C, 1.B.1.a, 3.C.2, 3.C.3, 3.C.4, 3.C.7, 2.D.3, 2.B.9, 2.E, 2.F, 2.G) – oil refineries and transformation industry, & fuel exploitation, & coal production, & agricultural soils, & solvents and products use; "7" represents all "groups" summed together
ower_Uncertainties_Percentage_0.1_0.1	file has 2×8×12 fields with monthly upper and lower uncertainty bounds in percent per emission "group" and for all "groups" summed together on a regular grid with 1800 pixels along the latitude and 3600 pixels along the longitude, where values represent centre of the grid-cell	file structure is identical to the file Annual_Upper_Lower_Uncertainties_Percentage_0.1_0.1.nc, but per month (1, 2, …, 12 correspond to January, February, …, December)
Annual_Upper_Lower_Uncertainties_0.1_0.1.nc	file has 3×8 fields with annual emissions, and upper and lower uncertainty bounds in kg·m^{-2}·s^{-1} per emission "group" and for all "groups" summed together on a regular grid with 1800 pixels along the latitude and 3600 pixels along the longitude, where values represent centre of the grid-cell	"Sup_lower" – lower uncertainty bound (2.5th percentile of log-normal distribution) for yearly emissions of ENERGY_S, in kg·m^{-2}·s^{-1}, "Sup_upper" – upper uncertainty bound (97.5th percentile of log-normal distribution) for yearly emissions of ENERGY_S, in kg·m^{-2}·s^{-1}, "Sup_flux" – yearly emissions of ENERGY_S, in kg·m^{-2}·s^{-1}
		"Ene_lower", "ene_upper", "ene_flux" – same, but for ENERGY_A, in kg·m^{-2}·s^{-1}
		"Man_lower", "man_upper", "man_flux" – same, but for MANUFACTURING, in kg·m^{-2}·s^{-1}
		"Set_lower", "set_upper", "set_flux" – same, but for SETTLEMENTS, in kg·m^{-2}·s^{-1}
		"Avi_lower", "avi_upper", "avi_flux" – same, but for AVIATION, in kg·m^{-2}·s^{-1}
		"Tra_lower", "tra_upper", "tra_flux" – same, but for TRANSPORT, in kg·m^{-2}·s^{-1}
		"Oth_lower", "oth_upper", "oth_flux" – same, but for OTHER, in kg·m^{-2}·s^{-1}
		"All_lower", "all_upper", "all_flux" – same, but for all "groups" summed together, in kg·m^{-2}·s^{-1}
Monthly_Sup_Upper_Lower_Uncertainties_	file has 3×12 fields with monthly emissions, and upper and lower uncertainty bounds in kg·m^{-2}·s^{-1} per ENERGY_S emission "group" on a regular grid with 1800 pixels along the latitude and 3600 pixels along the longitude, where values represent centre of the grid-cell	"Sup_lower" – lower uncertainty bound (2.5th percentile of log-normal distribution) for monthly emissions of ENERGY_S, in kg·m^{-2}·s^{-1}
		"Sup_upper" – upper uncertainty bound (97.5th percentile of log-normal distribution) for monthly emissions of ENERGY_S, in kg·m^{-2}·s^{-1}
		"Sup_flux" – monthly emissions of ENERGY_S, in kg·m^{-2}·s^{-1}
		"Month" – month numerical name, where 1, 2, …, 12 correspond to January, February, …, December

Monthly_Ene_Upper_Lower_Uncertainties_0.1_0.1.nc	file has 3×12 fields with monthly emissions, and upper and lower uncertainty bounds in $kg \cdot m^{-2} \cdot s^{-1}$ per ENERGY_A emission "group" on a regular grid with 1800 pixels along the latitude and 3600 pixels along the longitude, where values represent centre of the grid-cell	file structure is identical to the file Monthly_Sup_Upper_Lower_Uncertainties_0.1_0.1.nc, but with "ene_lower", "ene_upper", "ene_flux" fields
Monthly_Man_Upper_Lower_Uncertainties_0.1_0.1.nc	file has 3×12 fields with monthly emissions, and upper and lower uncertainty bounds in $kg \cdot m^{-2} \cdot s^{-1}$ per MANUFACTURING emission "group" on a regular grid with 1800 pixels along the latitude and 3600 pixels along the longitude, where values represent centre of the grid-cell	file structure is identical to the file Monthly_Sup_Upper_Lower_Uncertainties_0.1_0.1.nc, but with "man_lower", "man_upper", "man_flux" fields
Monthly_Set_Upper_Lower_Uncertainties_0.1_0.1.nc	file has 3×12 fields with monthly emissions, and upper and lower uncertainty bounds in $kg \cdot m^{-2} \cdot s^{-1}$ per SETTLEMENTS emission "group" on a regular grid with 1800 pixels along the latitude and 3600 pixels along the longitude, where values represent centre of the grid-cell	file structure is identical to the file Monthly_Sup_Upper_Lower_Uncertainties_0.1_0.1.nc, but with "set_lower", "set_upper", "set_flux" fields
Monthly_Avi_Upper_Lower_Uncertainties_0.1_0.1.nc	file has 3×12 fields with monthly emissions, and upper and lower uncertainty bounds in $kg \cdot m^{-2} \cdot s^{-1}$ per AVIATION emission "group" on a regular grid with 1800 pixels along the latitude and 3600 pixels along the longitude, where values represent centre of the grid-cell	file structure is identical to the file Monthly_Sup_Upper_Lower_Uncertainties_0.1_0.1.nc, but with "avi_lower", "avi_upper", "avi_flux" fields
Monthly_Tra_Upper_Lower_Uncertainties_0.1_0.1.nc	file has 3×12 fields with monthly emissions, and upper and lower uncertainty bounds in $kg \cdot m^{-2} \cdot s^{-1}$ per TRANSPORT emission "group" on a regular grid with 1800 pixels along the latitude and 3600 pixels along the longitude, where values represent centre of the grid-cell	file structure is identical to the file Monthly_Sup_Upper_Lower_Uncertainties_0.1_0.1.nc, but with "tra_lower", "tra_upper", "tra_flux" fields
Monthly_Oth_Upper_Lower_Uncertainties_0.1_0.1.nc	file has 3×12 fields with monthly emissions, and upper and lower uncertainty bounds in $kg \cdot m^{-2} \cdot s^{-1}$ per OTHER emission "group" on a regular grid with 1800 pixels along the latitude and 3600 pixels along the longitude, where values represent centre of the grid-cell	file structure is identical to the file Monthly_Sup_Upper_Lower_Uncertainties_0.1_0.1.nc, but with "oth_lower", "oth_upper", "oth_flux" fields
Monthly_All_Upper_Lower_Uncertainties_0.1_0.1.nc	file has 3×12 fields with monthly emissions, and upper and lower uncertainty bounds in $kg \cdot m^{-2} \cdot s^{-1}$ for all "groups" summed together on a regular grid with 1800 pixels along the latitude and 3600 pixels along the longitude, where values represent centre of the grid-cell	file structure is identical to the file Monthly_Sup_Upper_Lower_Uncertainties_0.1_0.1.nc, but with "all_lower", "all_upper", "all_flux" fields
CHE_EDGAR_2015.xlsx	file has 16 spreadsheets with listed information per country (metadata, emissions, uncertainties, statistical parameters)	"COUNTRY" – ISO Code (3-letter abbreviation of a geographical entity), Geographical name (name of a geographical entity), Type (development level of country's statistical infrastructure, meaning with well-/less well-developed statistical infrastructure), Main country (dependency, which country geographical entity in question belongs to), Full information (full name of a geographical entity, and what territory it occupies on the map of this study)

		"GROUP" – № (number of anthropogenic CO_2 emission "group"), group ("group" name), IPCC (2006) activity (IPCC activities that are included in each "group"), Note (short explanation of the "group"), Global emission budget 2015, Mt (total global emissions per "group"), Prior uncertainty bounds, % (initial, calculated purely based on assumptions from IPCC, lower and upper uncertainty bounds for country's with well-/less well-developed statistical infrastructures)
		"YEARLY" – ISO Code (3-letter abbreviation of a geographical entity), group ("group" name), Budget, kt (yearly anthropogenic CO_2 emission budget per "group" and total per geographical entity), Uncertainty bounds, % (calculated based on Prior uncertainty bounds and Budgets yearly uncertainties per "group" and total per geographical entity, uncertainties lower/upper/average bounds), Contribution to total country's uncertainty, % (share of each "group" in geographical entities total yearly uncertainty, total contribution is always 100 %), Parameters of log-normal distribution (anthropogenic CO_2 emission distribution is assumed to be log-normal, so additionally for modelling purposes log-normal mean, log-normal standard deviation and log-normal variance were calculated)
		"MONTHLY_01", "MONTHLY_02", …, "MONTHLY_12" – same explanation as for spreadsheet "YEARLY", but for a month (01, 02, …, 12 correspond to January, February, …, December)

3.4 Example of uncertainty calculation

Table 4 shows a step-by-step example of how yearly uncertainties are calculated, and Figure 2 shows plotted probability density functions based on computed log-normal parameters. The example shows calculations for the TRANSPORT "group", that consists of several emission "sectors". The example shows two countries with different statistical infrastructure development levels (country with well-developed statistical infrastructure is Germany, country with less well-developed statistical infrastructure is the Russian Federation) and significant differences in emission budgets.

Table 4a: Preparatory step for yearly uncertainty calculation – data collection, same values are applied for all countries of the same type, namely for countries with well- (WDS) and less well-developed (LDS) statistical infrastructures; example shows TRANSPORT "group" uncertainty calculations for Germany (DEU) and the Russian Federation (RUS)

IPCC (2006) activities per "sector"	IPCC (2006) activity	Note	Typical fuel	Uncertainty, %							
				Emission factor				Activity data			
				DEU (WDS)		RUS (LDS)		DEU (WDS)		RUS (LDS)	
				Low	Up	Low	Up	Low	Up	Low	Up
1.A.3.b	1.A.3.b	Road transportation	most typical emission factor	2.0	2.0	5.0	5.0	5.0	5.0	5.0	5.0
1.A.3.d	1.A.3.d	Water-borne navigation	composition of 80 % diesel and 20 % residual fuel oil	2.1	1.1	2.1	1.1	5.0	5.0	50.0	50.0
1.A.3.c, 1.A.3.e	1.A.3.c	Railways	diesel	2.0	0.9	2.0	0.9	5.0	5.0	5.0	5.0
	1.A.3.e	Other transportation – Pipeline	none (suggested to neglect)	0.0	0.0	0.0	0.0	0.0	0.0	0.0	0.0
		Other transportation – Off-road	most typical emission factor	2.0	2.0	5.0	5.0	50.0	100.0	50.0	100.0

Table 4b: First part of yearly uncertainty calculation – same values are applied for all countries of the same type, namely for countries with well- (WDS) and less well-developed (LDS) statistical infrastructures; example shows TRANSPORT "group" uncertainty calculations for Germany (DEU) and the Russian Federation (RUS)

IPCC (2006) activities per "sector"	IPCC (2006) activity	Combined uncertainty per IPCC (2006) activity, % see Eq. (1)				Combined uncertainty per "sector", % see Eq. (2)				Corrected combined uncertainty per "sector", % see Eq. (3)-(4)			
		DEU (WDS)		RUS (LDS)		DEU (WDS)		RUS (LDS)		DEU (WDS)		RUS (LDS)	
		Low	Up	Low	Up	Low	Up	Low	Up	Low	Up	Low	Up
1.A.3.b	1.A.3.b	5.4	5.4	7.1	7.1	5.4	5.4	7.1	7.1	5.4	5.4	7.1	7.1
1.A.3.d	1.A.3.d	5.4	5.1	50.0	50.0	5.4	5.1	50.0	50.0	5.4	5.1	50.0	50.0
1.A.3.c, 1.A.3.e	1.A.3.c	5.4	5.1	5.4	5.1	50.3	100.1	50.5	100.3	50.3	106.9	50.5	107.0
	1.A.3.e	0.0	0.0	0.0	0.0								
		50.0	100.0	50.2	100.1								

Table 4c: Second part of yearly uncertainty calculation – values are specific per geographical entity, consider country type, namely if country has well- (WDS) or less well-developed (LDS) statistical infrastructure, and countries emission budget (values are from CHE_EDGAR-ECMWF_2015); example shows TRANSPORT "group" uncertainty calculations for Germany (DEU) and the Russian Federation (RUS); "St. Dev." stands for standard deviation

IPCC (2006) activities per "sector"	Emission budget 2015 per "sector", $\cdot 10^3$ kt		Uncertainty with assumed log-normal distribution per "sector", %				Emission budget 2015 per "group", $\cdot 10^3$ kt see Eq. (6)		Grouped uncertainty with assumed log-normal distribution per "group", % see Eq. (5)				Log-normal parameters of grouped uncertainty with assumed log-normal distribution per "group" see Eq. (9)-(10)			
	DEU (WDS)	RUS (LDS)	DEU (WDS)		RUS (LDS)		DEU (WDS)	RUS (LDS)	DEU (WDS)		RUS (LDS)		DEU (WDS)		RUS (LDS)	
			Low	Up	Low	Up			Low	Up	Low	Up	Mean	St.Dev.	Mean	St.Dev.
1.A.3.b	139.6	131.7	5.4	5.4	7.1	7.1	143.0	206.9	5.3	5.7	14.1	44.8	11.9	0.0	12.3	0.1
1.A.3.d	1.0	7.4	5.4	5.1	40.1	57.2										
1.A.3.c, 1.A.3.e	2.3	67.9	40.3	135.5	40.5	135.7										

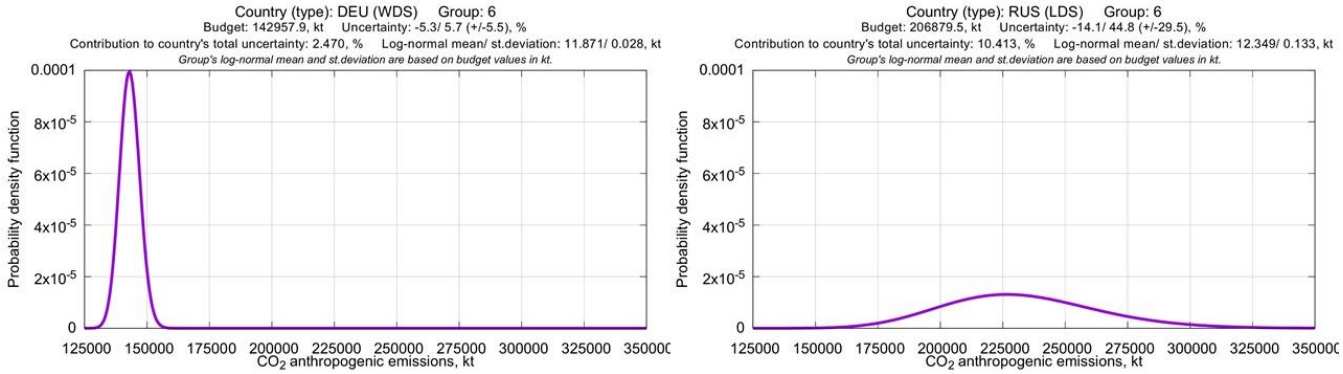

Figure 2: Probability density functions (for Germany (left) and the Russian Federation (right)) based on computed log-normal mean and standard deviation for TRANSPORT "group"

Calculated yearly and monthly uncertainties per country and emission "group" were assigned to each grid-box on the global map. National uncertainties were applied uniformly across each country. Figure 3 shows an example of the upper and lower uncertainty limits of anthropogenic CO_2 emission flux for the TRANSPORT "group". It should be noted that uncertainties related to the spatial distribution (representativeness of the proxy data and their uncertainty) should be much higher than the

ones presented in this study. This research does not address uncertainties related to the spatial distribution. In the future it is planned to address these uncertainties too. For example, by following Oda et al. (2019) to characterize spatial patterns of the disaggregation errors in the emission maps.

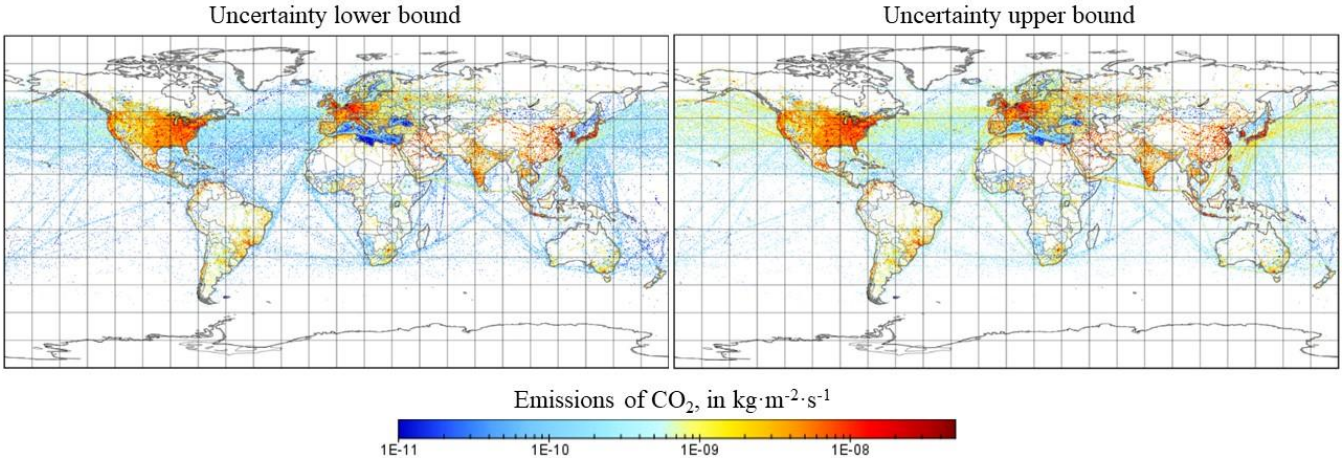

Figure 3: CO_2 emission flux uncertainties (lower (left) and upper (right) bounds) for TRANSPORT "group" in kg·m^{-2}·s^{-1}

4 Comparison and sensitivity

4.1 Comparison of total uncertainty of global CO_2 emission datasets

Calculated emissions and uncertainties of fossil CO_2 have been compared to other global data sets based on the country-specific data reported to UNFCCC, and on fuel-specific data reported in the energy statistics of IEA. The global values and their uncertainty at a 2σ range for the CHE_EDGAR-ECMWF_2015 dataset show the lowest value of -4.7/+9.6 % or ±7.1 % range, see Table 5. This result might be attributed to the methodology, in particular considering that (i) all calculations were done at the country level and then aggregated to global level assuming no correlation following IPCC (2006), (ii) all calculations were done separately for upper and lower uncertainty bounds to preserve original information with asymmetric confidence intervals for large uncertainties (not required for the Approach 1 described in IPCC (2006), in which only the higher uncertainty value of the asymmetric interval should be used – leads to artificial inflation of uncertainty upper or lower limit), and (iii) might be also because in this study proxy grid-map uncertainties are not considered.

Table 5: Comparison of global anthropogenic CO_2 emission uncertainty at 2σ associated with certain emission datasets

Name	Global uncertainty at 2σ, %	References
BP	no quantitative assessment of uncertainty associated with its emissions dataset	Andrew, 2020
CDIAC	±8.4 %	Andres et al., 2016

CEDS	no quantitative assessment of uncertainty associated with its emissions dataset	Hoesly et al., 2018
CHE_EDGAR-ECMWF_2015	*±7.1 % (-4.7/+9.6 %)*	*Current study*
EDGAR	±9.0 %	Janssens-Maenhout et al., 2019
EIA	no quantitative assessment of uncertainty associated with its emissions dataset	Andrew, 2020
Global Carbon Project (GCP)	±10.0 %	Friedlingstein et al., 2019
IEA	no quantitative assessment of uncertainty associated with its emissions dataset	Andrew, 2020
ODIAC	±8.4 %[3]	Oda et al., 2018

The contribution of each emission "group" to the total uncertainty per grid-cell is assessed. Figures 4-7 show which "group" contributes the most to the total uncertainty per grid-cell. TRANSPORT "group" contributes most to the grid-cell uncertainty over the Unites States of America (due to road and off-road transport) and over the ocean (due to shipping). AVIATION "group" contributes most over main flight routes all over the Globe. OTHER "group" contributes the most over agricultural areas, and regions with oil refineries and transformation industry and fuel exploitation. MANUFACTURING "group" contributes most over industrial areas (e.g. in Vietnam and Bangladesh). ENERGY_A (and ENERGY_S) "group" contributes the most over power plant (and super power plant) location grid-cells (e.g. South Africa). SETTLEMENT "group" contributes the most to the grid-cell uncertainty over either very dense, either very sparce populated areas.

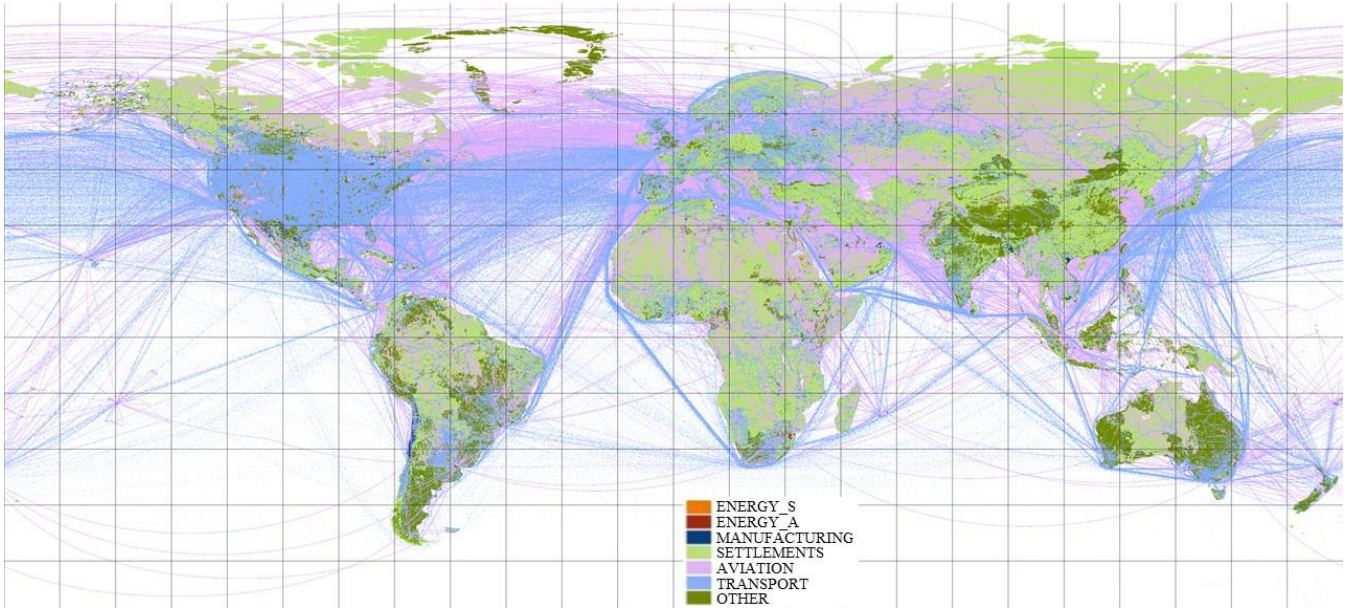

Figure 4: Main emission "group" that contributes to the total uncertainty per grid-cell – Global region

[3] The difference between ODIAC and CDIAC gridded data is 3.3-5.7 % (Oda et al., 2018).

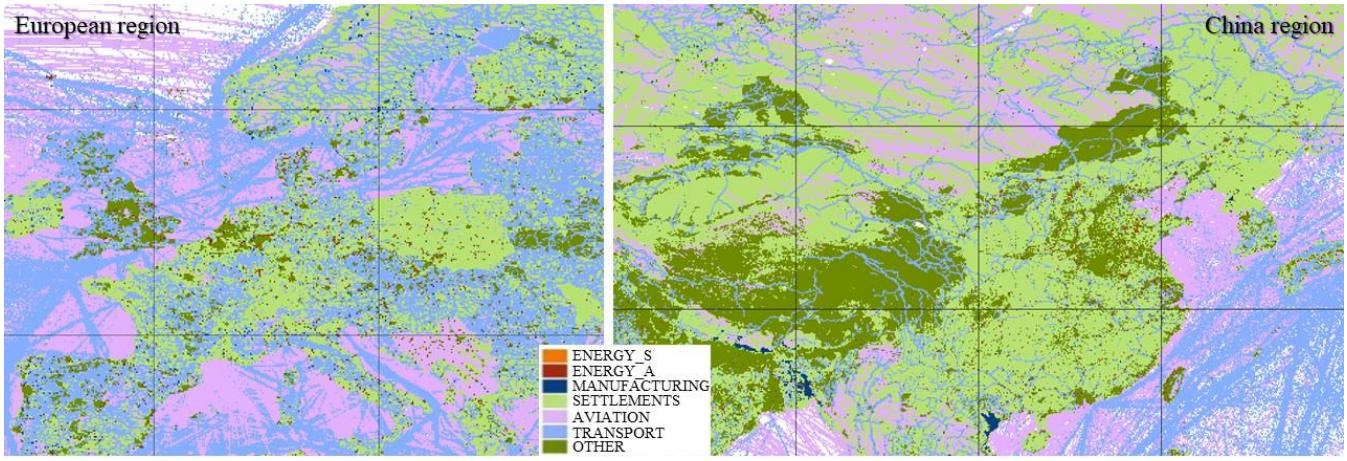

Figure 5: Main emission "group" that contributes to the total uncertainty per grid-cell – European (left) and China (right) regions

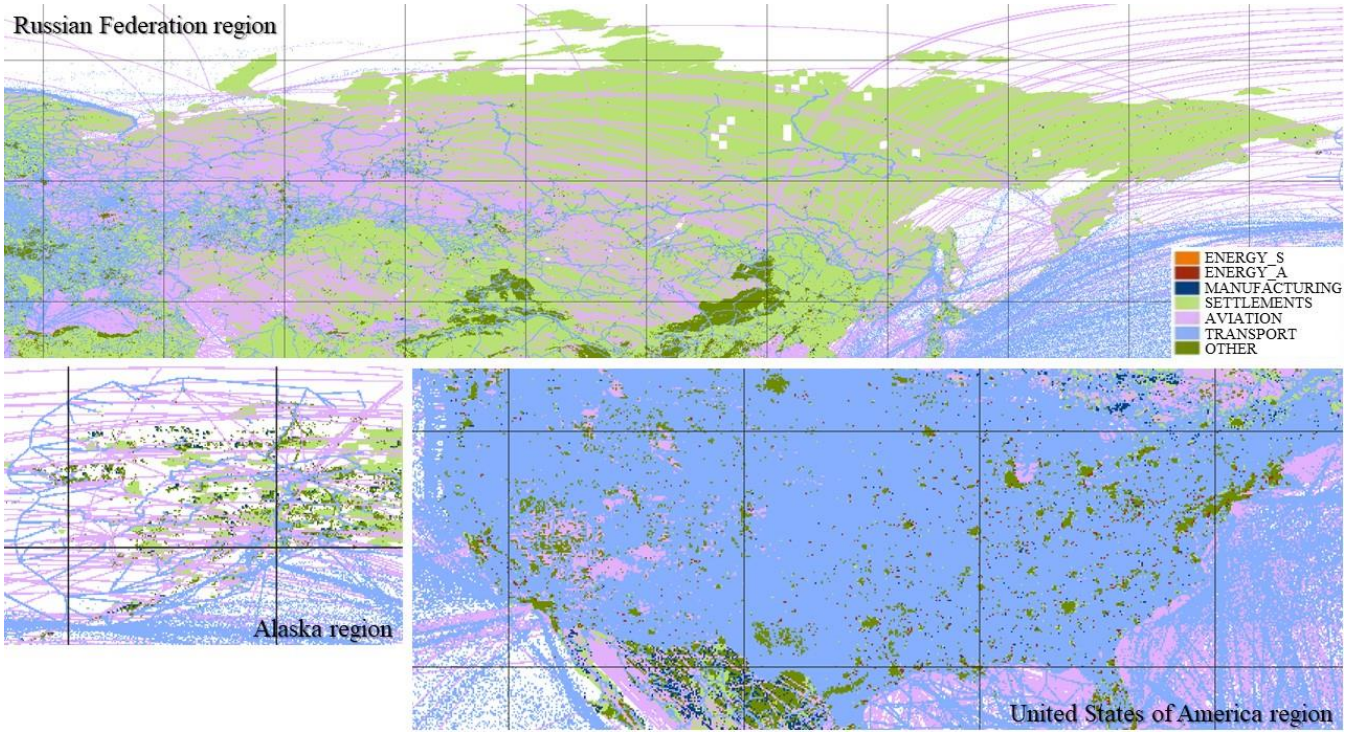

Figure 6: Main emission "group" that contributes to the total uncertainty per grid-cell – the Russian Federation (top) and the United States of America (bottom) regions

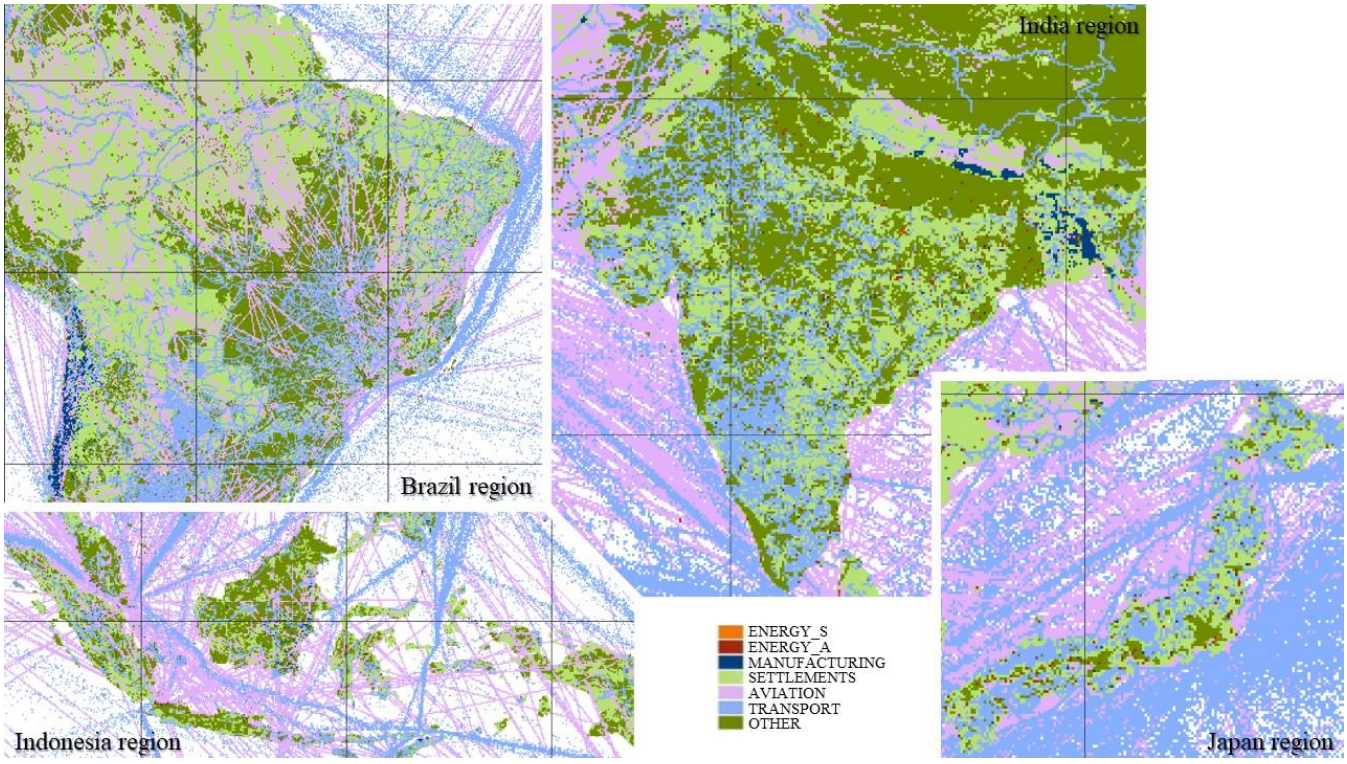

Figure 7: Main emission "group" that contributes to the total uncertainty per grid-cell – Brazil (top left), India (top right), Indonesia (bottom left), and Japan (bottom right) regions

355

4.2 Dependence of the country-specific statistical infrastructure

Also, some specific geographical areas are analysed: chosen to be among the most emitting in total or per emission "group", and the most typical or most influential for a certain region. A list of these geographical entities and development levels of their statistical infrastructures are presented in Table 6.

360

Table 6: List of selected geographical entities with their statistical infrastructure's development levels

ISO Code	Geographical name	Type
GLB	All World Countries	mixed-developed statistical infrastructure
E28	Europe (28 members until end 2019)	well-developed statistical infrastructure
DEU	Germany	well-developed statistical infrastructure
ESP	Spain	well-developed statistical infrastructure
FRA	France	well-developed statistical infrastructure
GBR	United Kingdom	well-developed statistical infrastructure
POL	Poland	well-developed statistical infrastructure
BRA	Brazil	less well-developed statistical infrastructure
CHN	China	well-developed statistical infrastructure
IDN	Indonesia	less well-developed statistical infrastructure

IND	India	well-developed statistical infrastructure
JPN	Japan	well-developed statistical infrastructure
RUS	Russian Federation	less well-developed statistical infrastructure
USA	United States of America	well-developed statistical infrastructure

In order to see how the development level of country's or geographical entity's statistical infrastructure influences the emission uncertainty of that country or geographical entity itself and (possibly) the globe, uncertainty calculations for selected entities were performed twice – with their original and switched types (i.e. a country with a well-developed statistical infrastructure becomes a country with a less well-developed statistical infrastructure and vice versa). More details on a geographical entity's statistical infrastructure development level (e.g. how it was determined) are given in the Supplementary Information, section S.5. Figure 8 shows sectoral emission budgets, uncertainties and contributions in percentage, to the total uncertainty of a country or geographical entity with its original and switched statistical infrastructure development levels. The biggest impact of development level change occurs for countries with larger emission budgets. On average, total uncertainties of selected countries (see Table 6) changed by 1-2 %; "group" uncertainties changed in line with prior uncertainties and countries emission budgets, as reported in Table 7.

Table 7: Country's statistical infrastructure (countries with well- (WDS) and less well-developed (LDS) statistical infrastructures) influence on emission uncertainty

Impact on the uncertainty	"Group" name	Cause description
most substantial	SETTLEMENTS	• consists only from residential heating emissions; • high differences in prior uncertainties for WDS and LDS, ±12.2 % and ±26.0 % respectively
strong	MANUFACTURING	• budget usually makes a significant part of country's total emission budget; • globally mainly composed from combustion for manufacturing with rather low prior uncertainty (±8.6 % and ±12.2 % for WDS and LDS respectively) and non-metallic minerals production with much higher uncertainties (±70.9 % and ±93.0 % for WDS and LDS respectively); • also contains emissions from very uncertain non-energy use of fuels (±121.7 % and ±124.0 % for WDS and LDS respectively) and chemical processes (-107.8/+89.9 % both for WDS and LDS) emissions, though their global share in this "group" is only ~7.0 %
	ENERGY_A	• budget usually makes a significant part of country's total emission budget; • composed of emissions from standard power plants with rather low uncertainties (±8.6 % and ±12.2 % for WDS and LDS respectively) and solid waste incineration with much higher uncertainties (±40.3 % and ±41.2 % for WDS and LDS respectively); • for the Globe the ratio of solid waste incineration to energy emissions is ~1/100, which keeps the total "group" prior uncertainty quite low ±3.5 %; • Note: geographical entities with higher ratios will have higher uncertainties
	ENERGY_S	• composed of emissions from super power plants only with rather low prior uncertainties (-8.6/+3.0 % and -12.2/+3.0 % for WDS and LDS respectively) for all geographical entities
mild	TRANSPORT	• globally mainly composed of road transportation with rather low uncertainty (±5.4 % and ±7.1 % for WDS and LDS respectively) and shipping emissions with low uncertainties -5.4/+5.1 % for WDS and high uncertainties ±50.0 % for LDS; • also contains rather uncertain railways, pipelines and off-road transport emissions (~ -50.4/+107.0 % for both WDS and LDS), though their global share in this "group" is ~16.0 % only; • Note: all international shipping is included in All World Countries geographical entity

small	AVIATION	• extremely high differences in prior uncertainties for WDS and LDS (-5.5/+6.4 % and -50.1/+106.8 % respectively), though this "groups" share in global emissions is only 2.3 %; • Note: all international aviation is included in All World Countries geographical entity
negligible	OTHER	• composed of very uncertain components with usually almost the same prior uncertainties for WDS and LDS; • main composite globally (~78.0 %) are emissions from oil refineries and transformation industry with prior uncertainties -54.4/+149.3 % and -57.7/+151.4 % for WDS and LDS respectively; • also usually has the highest contribution to the country's total uncertainty

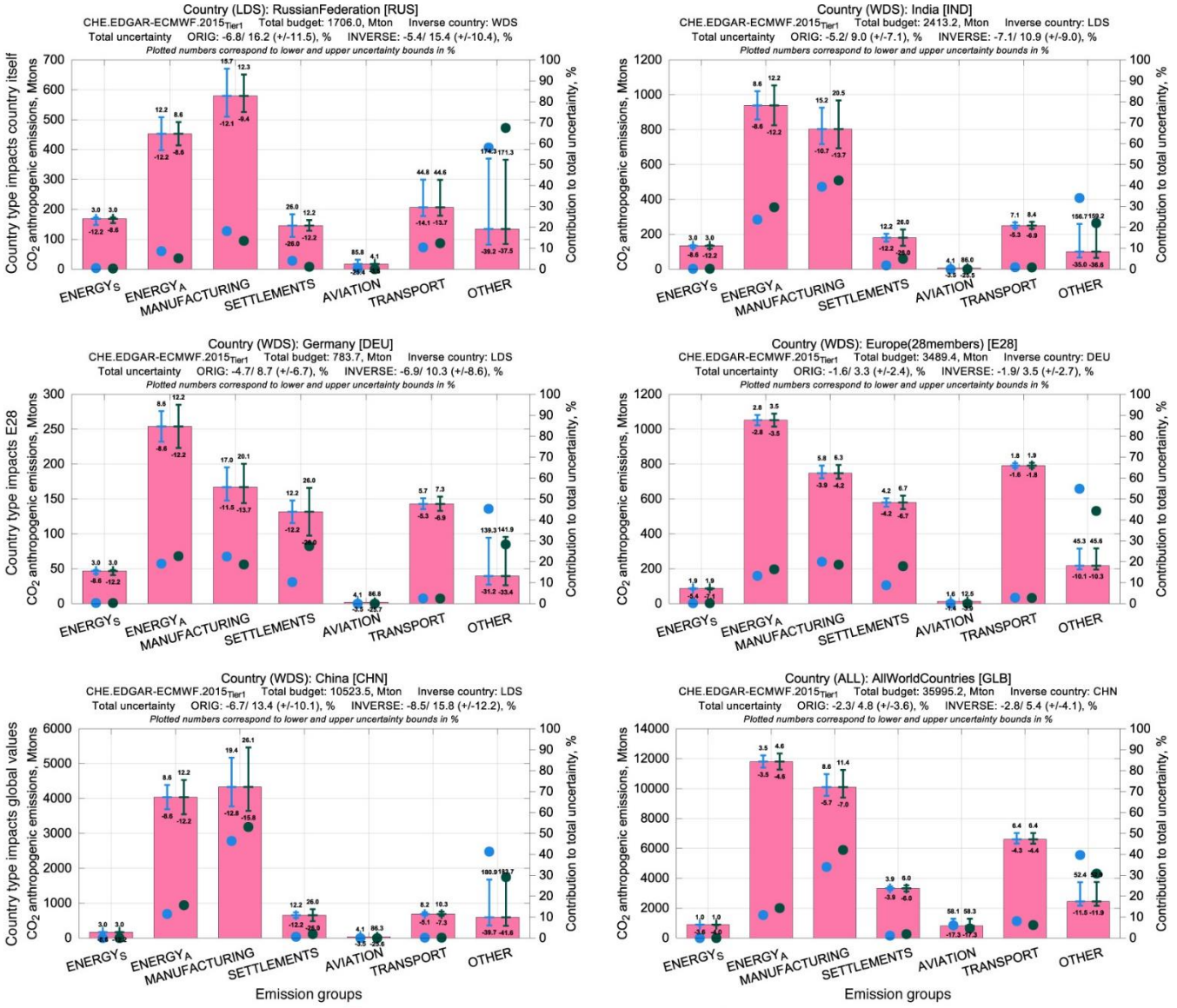

Figure 8: Emission budgets, uncertainties and contributions in percentage to the total uncertainty of the country with their original and switched (inverse) types (countries with well- (WDS) and less well-developed (LDS) statistical infrastructures): impacting mainly country itself, e.g. the Russian Federation (RUS), India (IND), impacting also Europe (E28), e.g. Germany (DEU), impacting even global values, e.g. China (CHN)

Alterations in some countries' (e.g. Germany, France) statistical infrastructure's development levels lead to changes in Europe (28 members until end 2019) uncertainties, with the most substantial change for the SETTLEMENTS "group" (e.g. 2.5 and 1.0 % respectively). Huge changes (> 10.0 %) in Europe's (28 members until end 2019) AVIATION "group" uncertainty percentage value can be due to the variation of statistical infrastructure development level for Germany, United Kingdom, France or Spain; though this "group's" contribution to Europe's total uncertainty remains negligible. Alterations in statistical infrastructure development levels for China or the United States of America, modify even global uncertainties because these countries substantially contribute to the total global emission budget, e.g. China emits ~1/3 of the global anthropogenic CO_2 budget and can change global total uncertainty up to 0.5 %.

4.3 Effect of increasing temporal resolution from yearly to monthly

To increase the emission temporal resolution, monthly emissions and their uncertainties were calculated combining yearly emissions, monthly multiplication factors, and adapted uncertainty calculation methodology (see Section 2.2). Prior yearly uncertainties were multiplied by a dimensionless uncertainty boosting parameter α (same value for each month) to compute prior monthly uncertainties, which were further used together with monthly emission budgets for countries' monthly uncertainty calculation. Monthly uncertainties (just like yearly uncertainties) are determined by empirical formulas from IPCC (2006) with monthly emission budgets (weighted with the total number of days in a month). The dimensionless uncertainty boosting parameter α is applied, see Table 8 for most common values for countries with well- and less well-developed statistical infrastructures per "sector". Boosting parameters become active ($\alpha \neq 1$), when absolute uncertainty values are ≥ 25.0 %, and α increases with the increase of absolute uncertainty following a third order polynomial. For lower bound uncertainties, α has larger values and steeper growth than for upper bound uncertainties (e.g. -25.0 % ≙ α = 1.5 and -124.0 % ≙ α = 2.6; +25.0 % ≙ α = 0.8 and +124.0 % ≙ α = 1.2; ≙ means "corresponds to"), and α behaves in the same way for countries with well- and less well-developed statistical infrastructures. Discrepancies in a different geographical entity's (country's) boosting parameters might be for several reasons, main ones are: (i) "sector" emissions were zero (e.g. super power plant emissions of the energy "sector" had no emissions); (ii) "sector" uncertainties were ≥ 50.0 % and needed to be adapted accordingly to log-normal distribution (e.g. this is the case for the agricultural soils "sector" with prior uncertainties -70.7/+0.0 % both for countries with well- and less well-developed statistical infrastructures; discrepancies from Table 8 for agricultural soils are France α = 1.8/3.1, United Kingdom – 1.8/7.2, China – 1.8/8.4, Japan – 1.8/10.8, Brazil – 1.8/0.0, the Russian Federation – 1.8/5.6).

Table 8: Dimensionless (DN) boosting parameter uncertainties (lower and upper bounds) for countries with well- (WDS) and less well-developed (LDS) statistical infrastructures

№	"Group" name	IPCC (2006) activities per "sector"	Uncertainty boosting parameter, DN			
			WDS countries		LDS countries	
			Low	Up	Low	Up
1	ENERGY_S	1.A.1.a (subset)	1.0	1.0	1.0	1.0
2	ENERGY_A	1.A.1.a (rest)	1.0	1.0	1.0	1.0
		4.C	1.8	0.8	1.9	0.8
3	MANUFACTURING	1.A.2	1.0	1.0	1.0	1.0
		2.C.1, 2.C.2	1.7	0.8	1.7	0.8
		2.C.3, 2.C.4, 2.C.5, 2.C.6, 2.C.7	2.0	0.9	2.0	0.9
		2.D.1, 2.D.2, 2.D.4	2.6	1.2	2.6	1.2
		2.A.1, 2.A.2, 2.A.3, 2.A.4	2.0	0.9	2.3	1.0
		2.B.1, 2.B.2, 2.B.3, 2.B.4, 2.B.5, 2.B.6, 2.B.8	2.4	1.0	2.4	1.0
4	SETTLEMENTS	1.A.4, 1.A.5.a, 1.A.5.b.i, 1.A.5.b.ii	1.0	1.0	1.5	0.9
5	AVIATION	1.A.3.a_CRS	1.0	1.0	1.7	1.1
		1.A.3.a_CDS	1.0	1.0	1.7	1.1
		1.A.3.a_LTO	1.0	1.0	1.7	1.1
6	TRANSPORT	1.A.3.b	1.0	1.0	1.0	1.0
		1.A.3.d	1.0	1.0	1.7	0.9
		1.A.3.c, 1.A.3.e	1.7	1.1	1.7	1.1
7	OTHER	1.A.1.b, 1.A.1.c, 1.A.5.b.iii, 1.B.1.c, 1.B.2.a.iii.4, 1.B.2.a.iii.6, 1.B.2.b.iii.3	1.7	1.4	1.8	1.4
		1.B.2.a.ii, 1.B.2.a.iii.2, 1.B.2.a.iii.3, 1.B.2.b.ii, 1.B.2.b.iii.2, 1.B.2.b.iii.4, 1.B.2.b.iii.5, 1.C	3.0	2.4	3.1	2.5
		1.B.1.a	2.5	2.2	2.5	2.2
		3.C.2, 3.C.3, 3.C.4, 3.C.7	1.8	0.0	2.0	0.0
		2.D.3, 2.B.9, 2.E, 2.F, 2.G	1.5	0.8	1.7	0.9

In general, Brazil, Indonesia and India have a very weak yearly cycle with quite high monthly uncertainties throughout the year. Globe, Europe (28 members until end 2019), Germany, Spain, France, United Kingdom, Poland, China, Japan, the Russian Federation, and the United States of America have more pronounced yearly cycles, most significant for SETTLEMENTS and ENERGY_A (and ENERGY_S where present) "groups", and less significant for AVIATION, TRANSPORT and MANUFACTURING "groups". This is in line with the monthly profiles applied in EDGARv4.3.2 for Northern and Southern temperate zones, and Equator, see Janssens-Maenhout et al. (2019). In the summer months for the Northern temperate zone, a strong decrease in SETTLEMENT and ENERGY_A (and ENERGY_S where present) "groups" emissions was observed, with a light decrease in MANUFACTURING "group" emissions, and a light increase in AVIATION and TRANSPORT "groups" emissions. This corresponds rather well with the assumption that most of the population in the Northern hemisphere heat their houses during winter, and take holidays and travel more during summer.

4.4 Comparison for selected European countries with UNFCCC and TNO data

The CHE_EDGAR-ECMWF_2015 dataset containing 7 global gridded fossil CO_2 emission flux maps, and country- and "group"-specific emission budgets and uncertainties have been assessed with independent data. Global emission budget values from different datasets are almost never the same, therefore it is important to first identify why estimates differ between datasets. Datasets might use the same country-level information as primary input, though differences in inclusion, interpretation, and treatment of that data lead to diverse results in emissions. It is necessary to try to harmonise data inclusion or omission across datasets to have more clarity in the discrepancies.

For Europe (28 members until end 2019), Germany, Spain, France, United Kingdom, Poland, Japan, the Russian Federation and the United States of America, emission and uncertainty data was collected from UNFCCC NIR. The aggregation of the IPCC (2006) activity-specific emissions and uncertainties into 7 "groups" was done assuming no correlation, following IPCC (2006). Although IPCC (2006) has a standard table to report GHG emissions, uncertainties can be reported in less detail by a more general category (e.g. 2.D only instead of 2.D.1, 2.D.2, 2.D.3, 2.D.4), meaning information "harmonization" required lots of careful time-consuming country-specific technical work by the authors of this paper.

The Netherlands Organisation for Applied Scientific Research (TNO) has prepared the first version of their GHG and co-emitted species emission database (TNO_GHGco_v1.1) that covers the entire European domain (at $0.1^o \times 0.05^o$ resolution), including CO_2 (distinguishing between fossil fuel and biofuel). Initial emission data is from the UNFCCC (Common reporting format, CRF, tables) and the European Monitoring and Evaluation Programme/Centre on Emission Inventories and Projections for air pollutants (EMEP/CEIP). These data were harmonized, checked for gaps, errors and inconsistencies, and (where needed) replaced or completed using emission data from the Greenhouse gas-Air pollution Interactions and Synergies (GAINS) model (Amann et al., 2011). Moreover, inland shipping emissions were replaced with TNO's own estimates and sea shipping is based on automatic identification system (AIS) based tracks. Expert judgement is used to assess the quality of each data source and to make choices on which source to use. The resulting emissions were checked in detail regarding their absolute value and trends (Kuenen et al., 2014). In this study emission budgets from 30 TNO sectors (Super et al., February 2020, personal communication), and prior uncertainties calculated from IPCC (2006) and its refinements (IPCC, 2019) are used. In addition, TNO has provided Tier 2 (Monte Carlo approach) uncertainties based on the same budgets and uncertainties from submitted NIR reports based on a Tier 1 approach. The Monte Carlo simulations were done at the highest detail level (nomenclature for reporting (NFR) sector/fuel type) assuming correlations between certain sectors (for more information see Super et al. (2020)), and then emissions were aggregated to "groups" assuming no correlation.

Figure 9 shows emission budgets and uncertainties in megatonne, and contributions in percent to the total geographical entity's uncertainty for Europe (28 members until end 2019), Germany, France and United Kingdom with their original statistical infrastructure development types based on data from CHE_EDGAR-ECMWF_2015 (in pink), UNFCCC (in yellow), and TNO_GHGco_v1.1 Tier 1 (in blue) and Tier 2 (in green); plots for Spain and Poland are not shown here. Out of the four different sources, usually UNFCCC and TNO_GHGco_v1.1 Tier 2 uncertainties are the lowest ones and

CHE_EDGAR-ECMWF_2015 the highest one. It should be noted that: (i) UNFCCC uncertainties were aggregated to "groups" individually per country as uncertainties are reported in a rather free form, and thus could be aggregated from different levels of precision, (ii) uncertainties for Europe (28 members until end 2019) from CHE_EDGAR-ECMWF_2015 are rather low as they were calculated by aggregating information from 28 countries, and (iii) differences in uncertainties of CHE_EDGAR-ECMWF_2015 with other sources, especially in fuel dependent emission groups, might be due to biofuels or other fuels (e.g. wood and/or coal for residential heating). Differences in uncertainties between CHE_EDGAR-ECMWF_2015 and TNO_GHGco_v1.1 Tier 1 show additional value in more detailed emission budget knowledge (i.e. where absence of the uncertain glass production activity in the non-metallic minerals production "sector" decreases overall uncertainty). Differences in uncertainties between TNO_GHGco_v1.1 Tier 1 and TNO_GHGco_v1.1 Tier 2 show additional value in an advanced calculation technique, using a more sophisticated, data demanding Monte Carlo approach instead of simple error propagation. Overall, there is quite good agreement in emission budgets and uncertainties from different sources of emission data.

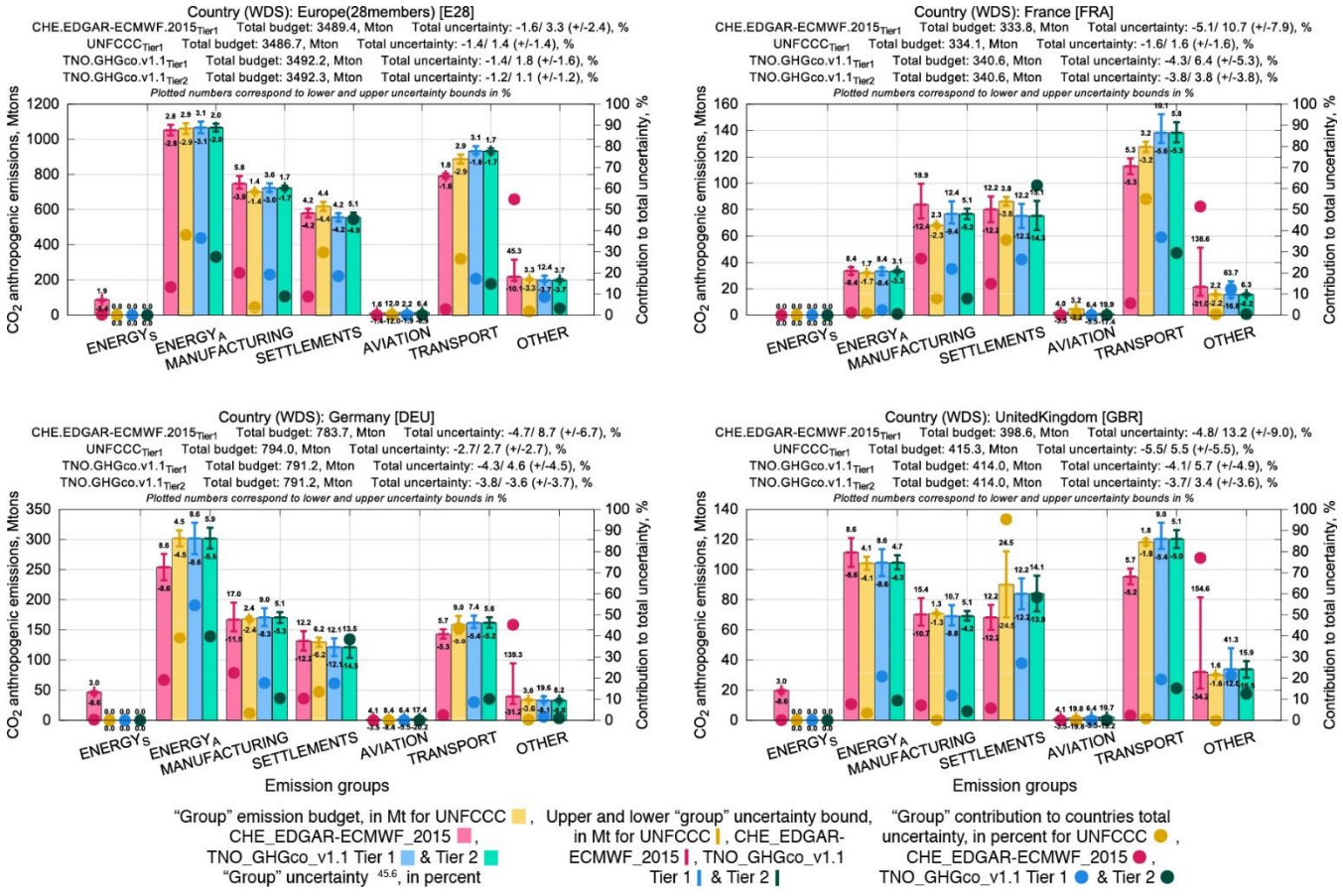

Figure 9: Emission budgets, uncertainties and contributions in percentage to the total uncertainty for Europe (E28), Germany (DEU), France (FRA) and United Kingdom (GBR)

Emission budgets, Tier 1 uncertainties, and contributions in percentage to the total geographical entity's uncertainty for Japan, the Russian Federation and the United States of America from CHE_EDGAR-ECMWF_2015 could be compared only with UNFCCC data (plots not shown here). UNFCCC uncertainties are usually lower than the ones calculated in this study. The main reason for that is the use of country-specific emission data and activity data uncertainties, which are lower than default values suggested by IPCC (2006) and its refinements (IPCC, 2019). Only for the fuel dependent "groups" (e.g. AVIATION) might UNFCCC uncertainties be higher than in this study, as rather uncertain biofuels might be taken into account (Note: CHE_EDGAR-ECMWF_2015 does not take biofuels into account). Also, emission budgets reported to UNFCCC show some differences from the ones from CHE_EDGAR-ECMWF_2015. For Japan, "group" budgets agree rather well, and the total budget difference is ~1.0 %. For the Russian Federation, major differences are in the ENERGY_A (and ENERGY_S) and MANUFACTURING "groups", which results in ~6.0 % higher total budget of CHE_EDGAR-ECMWF_2015. For the United States of America, major differences are ~200 Mt and ~100 Mt for the SETTLEMENTS and OTHER "groups" respectively, which results in ~4.0 % higher total budget than based on UNFCCC data. Recent comparison of different gridded global datasets by Andrew (2020) pointed out that only a few of these datasets provide quantitative uncertainty assessment, see the summary in Table 5. Compared to other global emission uncertainty values, CHE_EDGAR-ECMWF_2015 shows the lowest values mainly due to the aggregation technique.

4.5 Sensitivity to the fuel specificity

As mentioned above, for transport related emission uncertainty calculations only the most typical fuel type (for aviation, railways, shipping) and emission factor uncertainty (for road and off-road transport) were used, because detailed fuel consumption information per IPCC activity was not available for this study. The EDGAR dataset development team do have specific fuel information globally, which could be used for uncertainty calculation. The EDGAR dataset with incorporated fuel-specific activity data and emission factor uncertainties and Tier 1 approach for uncertainty calculation (see Supplementary Information, section S.6), is hereinafter referred to as EDGAR-JRC. Country budget uncertainties were calculated by considering "full fuel" splitting and by taking into consideration the assumption that the emission factors, from sectors sharing the same fuel, are fully correlated. This latter assumption transformed the sum in quadrature of Eq. (2) into a linear summation (Bond et al., 2004; Bergamaschi et al., 2015). The uncertainty of activity data was set in accordance with IPCC (2006) guidelines, in the range 5.0 to 10.0 % for combustion activities, 10.0 to 20.0 % for combustion in the residential sector, 25.0 % for bunker fuels in the marine transport, 35.0 % for industrial processes of cement, lime, glass, ammonia (the range of uncertainty values refers to the 95 % confidence interval of the mean, assigned separately to countries with well- and less well-developed statistical infrastructures). Uncertainties from EDGAR-JRC dataset aggregated to the "group" level were compared with the ones from CHE_EDGAR-ECMWF_2015, see Table 9 for Europe (28 members until end 2019) and

all world countries, and Table S8 from the Supplementary Information, section S.6, for all the rest geographical entities from Table 6. Emission uncertainties from EDGAR-JRC reflect the share of fuel composing the emission of each country and are in line with the estimates by CHE_EDGAR-ECMWF_2015 for those countries where the fuel-composite uncertainty is closer to the average value assigned. Uncertainties calculated with fuel-specific data are usually smaller; when prevailing fuel coincides with typical fuel type from CHE_EDGAR-ECMWF_2015 emission "group" uncertainties from both sources are quite similar. It should be noted that: (i) countries' total uncertainty is higher in EDGAR-JRC due to the aggregation technique (full correlation is assumed), (ii) AVIATION "group" uncertainties are higher in EDGAR-JRC due to prior aggregation of all three aviation connected sectors (cruise, climbing & descent, and landing & take off).

Table 9: Aggregated to the "group" level uncertainties (lower and upper bounds) in percent and contributions in percent to the total uncertainty (CV) for Europe (E28) and globe (GLB) from EDGAR-JRC (with extra fuel type knowledge) and CHE_EDGAR-ECMWF_2015 (with typical fuel only)

Country	"Group" name	EDGAR-JRC			CHE_EDGAR-ECMWF_2015		
		Low, %	Up, %	CV, %	Low, %	Up, %	CV, %
GLB	ENERGY_S	0.0	0.0	0.0	-3.6	1.0	0.0
	ENERGY_A	-2.9	2.7	42.4	-3.5	3.5	11.0
	MANUFACTURING	-4.3	4.3	41.3	-5.7	8.6	34.0
	SETTLEMENTS	-2.5	2.5	1.9	-3.9	3.9	1.1
	AVIATION	-4.2	5.8	0.5	-17.3	58.1	6.1
	TRANSPORT	-2.5	2.6	7.7	-4.3	6.4	8.1
	OTHER	-5.9	6.2	6.2	-11.5	52.4	39.7
	TOTAL	*-4.8*	*4.8*	*100.0*	*-2.3*	*4.8*	*100.0*
E28	ENERGY_S	0.0	0.0	0.0	-5.4	1.9	0.2
	ENERGY_A	-2.0	2.4	56.4	-2.8	2.8	13.3
	MANUFACTURING	-2.2	2.2	12.6	-3.9	5.8	20.0
	SETTLEMENTS	-2.5	2.5	15.1	-4.2	4.2	8.8
	AVIATION	-2.4	2.8	0.0	-1.4	1.6	0.0
	TRANSPORT	-1.3	1.3	7.2	-1.6	1.8	2.8
	OTHER	-5.0	5.0	8.7	-10.1	45.3	54.9
	TOTAL	*-3.3*	*3.6*	*100.0*	*-1.6*	*3.3*	*100.0*

The uncertainties derived in this study are an upper bound of the uncertainty estimation compared to the uncertainties calculated with more detailed information, as done by the countries and reported to UNFCCC or to the uncertainties calculated with fuel-specific data. Even though sometimes differences might be quite high in percentage values, they are usually quite small in megatonne.

4.6 Atmospheric sensitivity to nationally disaggregated emissions

The gridded emissions are required input to the ECMWF IFS model used to simulate atmospheric CO_2 globally (Agusti-Panareda et al., 2014; Agusti-Panareda et al., 2019). Ideally, uncertainties at a grid-cell level would be preferred by the models in general, which is a difficult time-consuming task. To check the usefulness of the information-intensive derivation of uncertainties at a grid-cell level, it was decided to run some experiments. High-resolution (~25 km horizontal resolution,

137 vertical levels) simulations with the ECMWF IFS model have been performed to assess the atmospheric sensitivity to fully resolved emissions compared to nationally smoothed (global emission budget is conserved), see Figure 10.

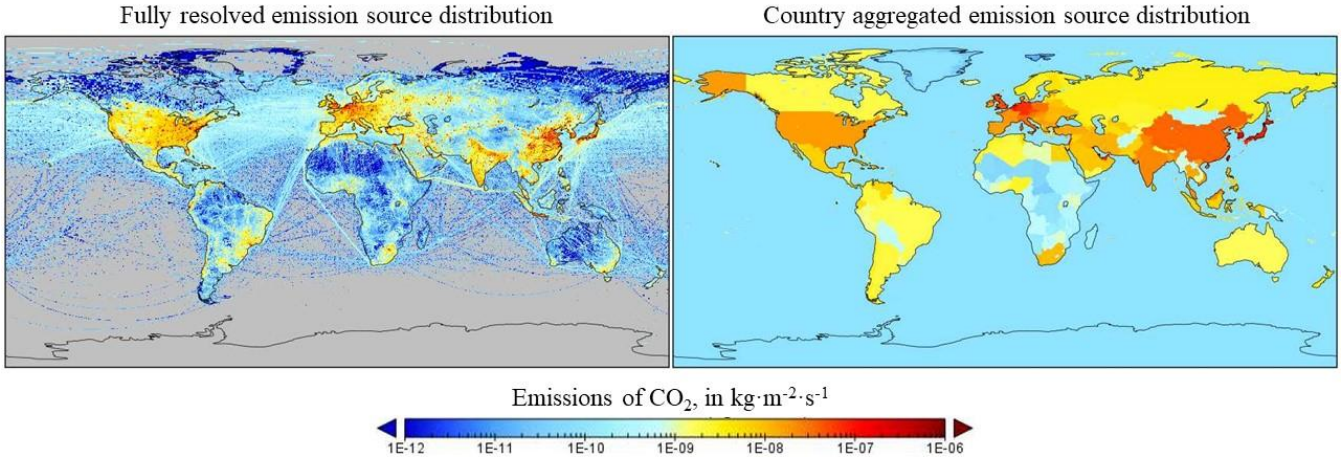

Figure 10: Anthropogenic CO_2 flux source distribution at ~25 km resolution – fully resolved (left), country aggregated (right)

Model simulations were performed for January 2015 with three hourly output. Anthropogenic, fire, ocean and biogenic fluxes (large-scale model bias mitigated by biogenic CO_2 flux adjustment scheme (BFAS)) were considered. For the full model configuration description see McNorton et al. (2020). It was noted that point sources (e.g. power plants, factories) can be easily detected if they comprise a substantial part of countries total emission budget (e.g. in South Africa). If point sources are distributed homogeneously over the country and other areal sources are rather high as well, it becomes difficult to detect one extra/missing emitting hotspot (e.g. in Germany). China is a very good example for both cases, as its western part has very few hotspots and they are easy to detect over the low emitting background. Its eastern part, however, has lots of hotspots and high emitting areal sources making it almost impossible to disentangle emissions from a single power plant or factory from the high emitting background. Differences of several ppm are detected over multiple regions, highlighting the importance of using high resolution spatially resolved emissions. With increase of both flux and transport model resolutions these differences are expected to increase further with steeper atmospheric CO_2 gradients.

5 Recommendations and conclusion

A pre-processor has been created that allows derivation of the upper and lower band uncertainty grid-maps, while making use of an appropriate classification of more certain and uncertain sectors. These grid-maps allow assessment of the error propagation of country emission budgets following the IPCC 2006 Guidelines for National Greenhouse Gas Inventories. It is a first step in evaluating where to provide more effort in reducing the propagated error budget that can be taken up in any

global or regional atmospheric model as a first step. The method has been applied using EDGARv4.3.2_FT2015 and was tested as input to the ECMWF IFS ensemble spread to characterise the carbon dioxide (CO_2) atmospheric concentrations' uncertainties in the prototype of the Copernicus CO_2 Monitoring and Verification Support Capacity. At country level the CHE_EDGAR-ECMWF_2015 dataset provides generally larger uncertainty ranges, reduced when more detailed information is available. In summary, using the information uniformly available for all countries, a coherent uncertainty representation is obtained.

The application in the ECMWF IFS Earth system model sheds light on the spatial representativeness of the emissions. While the emission-intensive point sources were checked with reference to their spatial location, the diffuse emission sources are gridded using spatial proxy data. With CHE_EDGAR-ECMWF_2015 implemented in the IFS model it was demonstrated that the choice of the spatial proxy data has a strong influence on the model results. As such, it is proposed that this is analysed in comparison to other datasets, going beyond the evaluation of the probability density of the spatial proxy itself. Contribution of representativeness errors to uncertainties and time correlation will need to be assessed in successive future studies, as foreseen under the Prototype system for a Copernicus CO_2 service ($CoCO_2$) project, following up on the CO_2 Human Emissions (CHE) project.

The use of ensemble technique to estimate CO_2 uncertainties is recommended. The optimal number of ensemble members is bounded by practical considerations on computational costs. Leutbecher (2018) found a minimum of 8-member ensemble can mimic some of the skill of larger ensembles, with a 20-member ensemble being a typical value used by several modelling systems and with 50-member being a desirable target. Further grouping of anthropogenic emissions into e.g. one to reduce the dimensions of the problem is also possible with the tool CHE_UNC_APP (Choulga et al., 2021).

The estimation of global gridded emissions with their spatially and temporally distributed uncertainties constitute the backbone for atmospheric inversions to estimate anthropogenic emissions from atmospheric concentrations (Pinty et al., 2017). Dedicated satellite missions (e.g. Copernicus anthropogenic CO_2 monitoring mission CO_2M described in Janssens-Maenhout et al. (2020)) are being planned to monitor anthropogenic emissions from space and substantially reduce emission uncertainties. The developments in the emission uncertainty, based on prior knowledge computation presented in this paper, are an important preparatory step for an ensemble-based CO_2 Monitoring and Verification System prototype, such as the one developed within the CHE project.

Data availability. EDGARv4.3.2 data are open access and available at http://edgar.jrc.ec.europa.eu/overview.php?v=432&SECURE=123, last access: 29 June 2021, doi:https://data.europa.eu/doi/10.2904/JRC_DATASET_EDGAR, documented in Janssens-Maenhout et al. (2019). CHE_EDGAR-ECMWF_2015 data (Choulga et al., 2020) are freely available https://doi.org/10.5281/zenodo.3967439, and documented in this paper. CHE_UNC_APP anthropogenic CO_2 emission uncertainty calculation tool (Choulga et al., 2021) is freely available https://doi.org/10.5281/zenodo.5196190, and documented in this paper.

Author contribution. All the authors participated in the uncertainty calculation tool CHE_UNC_APP design and CHE_EDGAR-ECMWF_2015 maps generation (methodology, data generation), model experiment set-up, and analysis of the result. Margarita Choulga and Greet Janssens-Maenhout wrote the manuscript with contributions from all the other authors.

Competing interests. The authors declare that they have no conflict of interest.

Acknowledgements. The authors thank Glenn Carver (ECMWF) for editorial help and assistance; Vladimir Tupoguz for invaluable support during the preparation of the paper and numerous discussions. Margarita Choulga was funded by the CO_2 Human Emissions (CHE) project which received funding from the European Union's Horizon 2020 research and innovation programme under grant agreement no. 776186, and by the Prototype system for a Copernicus CO_2 service ($CoCO_2$) project which received funding from the European Union's Horizon 2020 research and innovation programme under grant agreement no. 958927.

Financial support. This research has been supported by CHE (grant no. 776186) and CoCO2 (grant no. 958927).

References

Agustí-Panareda, A., Massart, S., Chevallier, F., Boussetta, S., Balsamo, G., Beljaars, A., Ciais, P., Deutscher, N.M., Engelen, R., Jones, L., Kivi, R., Paris, J.-D., Peuch, V.-H., Sherlock, V., Vermeulen, A.T., Wennberg, P.O., Wunch, D.: Forecasting global atmospheric CO_2, Atmos. Chem. Phys., 14, 11959-11983, https://doi.org/10.5194/acp-14-11959-2014, 2014.

Agustí-Panareda, A., Diamantakis, M., Massart, S., Chevallier, F., Muñoz-Sabater, J., Barré, J., Curcoll, R., Engelen, R., Langerock, B., Law, R.M., Loh, Z., Morguí, J.A., Parrington, M., Peuch, V.-H., Ramonet, M., Roehl, C., Vermeulen, A.T., Warneke, T., Wunch, D.: Modelling CO_2 weather – why horizontal resolution matters, Atmos. Chem. Phys., 19, 7347-7376, https://doi.org/10.5194/acp-19-7347-2019, 2019.

Amann, M., Bertok, I., Borken-Kleefeld, J., Cofala, J., Heyes, C., Höglund-Isaksson, L., Klimont, Z., Nguyen, B., Posch, M., Rafaj, P., Sandler, R., Schöpp, W., Wagner, F., Winiwarter, W.: Cost-effective control of air quality and greenhouse gases in Europe: Modelling and policy applications, Environmental Modelling and Software, Vol. 26, pp. 1489-1501, 2011.

Andres, R.J., Marland, G., Fung, I., and Matthews, E.: A 1° × 1° distribution of carbon dioxide emissions from fossil fuel consumption and cement manufacture, 1950-1990. Glob. Biogeochem. Cycles, 10, 419-429, https://doi.org/10.1029/96GB01523, 1996.

Andres, R.J., Boden, T.A., and Marland, G.: Annual Fossil-Fuel CO_2 Emissions: Mass of Emissions Gridded by One Degree Latitude by One Degree Longitude, United States: N. p., (NDP-058.2016), https://doi.org/10.3334/CDIAC/ffe.ndp058.2016, 2016.

Andrew, R.M: A comparison of estimates of global carbon dioxide emissions from fossil carbon sources, Earth Syst. Sci. Data, 12, 1437–1465, https://doi.org/10.5194/essd-12-1437-2020, 2020.

Asefi-Najafabady, S., Rayner, P.J., Gurney, K.R., McRobert, A., Song, Y., Coltin, K., Huang, J., Elvidge, C., Baugh, K.: A multiyear, global gridded fossil fuel CO_2 emission data product: Evaluation and analysis of results, J. Geophys. Res. Atmos., 119, 17, 10.213-10.231, https://doi.org/10.1002/2013JD021296, 2014.

Beamish, B.B., and Vance, W.E.: Greenhouse gas contributions from coal mining in Australia and New Zealand, Journal of the Royal Society of New Zealand, 22:2, 153-156, https://doi.org/10.1080/03036758.1992.10420812, 1992.

Bergamaschi, P., Corazza, M., Karstens, U., Athanassiadou, M., Thompson, R. L., Pison, I., Manning, A. J., Bousquet, P., Segers, A., Vermeulen, A. T., Janssens-Maenhout, G., Schmidt, M., Ramonet, M., Meinhardt, F., Aalto, T., Haszpra, L., Moncrieff, J., Popa, M. E., Lowry, D., Steinbacher, M., Jordan, A., O'Doherty, S., Piacentino, S., and Dlugokencky, E.: Top-down estimates of European CH4 and N2O emissions based on four different inverse models, Atmos. Chem. Phys., 15, 715–736, https://doi.org/10.5194/acp-15-715-2015, 2015.

Bond, T. C., Streets, D. G., Yarber, K. F., Nelson, S. M., Woo, J.-H., and Klimont, Z.: A technology-based Global inventory of black and organic carbon emissions from combustion, J. Geophys. Res.,109, D14203, doi:10.1029/2003JD003697, 2004.

CHE: CO_2 Human Emissions (CHE) project official website, available at: https://www.che-project.eu, last access: 29 June 2021.

Chen, H., Huang, Y., Shen, H., Chen, Y., Ru, M., Chen, Y., Lin, N., Su, S., Zhuo, S., Zhong, Q., Wang, X., Liu, J., Li, B., Tao, S.: Modelling temporal variations in global residential energy consumption and pollutant emissions, Applied Energy, 184, 0306-2619, 820-829, https://doi.org/10.1016/j.apenergy.2015.10.185, 2016.

Choulga, M., McNorton, J., Janssens-Maenhout, G.: CHE_EDGAR-ECMWF_2015 [Data set], Zenodo, https://doi.org/10.5281/zenodo.3967439, 2020.

Choulga, M., Janssens-Maenhout, G., McNorton, J.: Anthropogenic CO_2 emission uncertainty calculation tool CHE_UNC_APP [Software], Zenodo, https://doi.org/10.5281/zenodo.5196190, 2021.

Cong, R., Saitō, M., Hirata, R., Ito, A., and Maksyutov, S.: Uncertainty Analysis on Global Greenhouse Gas Inventories from Anthropogenic Sources, Proceedings of the 2nd International Conference of Recent Trends in Environmental Science and Engineering (RTESE'18), Niagara Falls, Canada 10-12.06.2018, Paper No. 141, https://doi.org/10.11159/rtese18.141, 2018.

Cong, R., Saitō, M., Hirata, R., Ito, A., and Maksyutov, S.: Uncertainty Analysis on Global Greenhouse Gas Inventories from Anthropogenic Sources, International Journal of Environmental Pollution and Remediation (IJEPR), Volume 7, Journal ISSN: 1929-2732, https://doi.org/10.11159/ijepr.2019.001, 2019.

Frey, H.C.: Evaluation of an Approximate Analytical Procedure for Calculating Uncertainty in the Greenhouse Gas Version of the Multi-Scale Motor Vehicle and Equipment Emissions System, Prepared for Office of Transportation and Air Quality, U.S. Environmental Protection Agency, Ann Arbor, MI, May 30, 2003.

Friedlingstein, P., Jones, M.W., O'Sullivan, M., Andrew, R.M., Hauck, J., Peters, G.P., Peters, W., Pongratz, J., Sitch, S., Le Quere, C., Bakker, D.C.E., Canadell, J.G., Ciais, P., Jackson, R.B., Anthoni, P., Barbero, L., Bastos, A., Bastrikov, V., Becker, M., Bopp, L., Buitenhuis, E., Chandra, N., Chevallier, F., Chini, L.P., Currie, K.I., Feely, R.A., Gehlen, M., Gilfillan, D., Gkritzalis, T., Goll, D.S., Gruber, N., Gutekunst, S., Harris, I., Haverd, V., Houghton, R.A., Hurtt, G., Ilyina, T., Jain, A.K., Joetzjer, E., Kaplan, J.O., Kato, E., Klein Goldewijk, K., Korsbakken, J.I., Landschutzer, P., Lauvset, S.K., Lefevre, N., Lenton, A., Lienert, S., Lombardozzi, D., Marland, G., McGuire, P.C., Melton, J.R., Metzl, N., Munro, D.R., Nabel, J.E.M.S., Nakaoka, S.-I., Neill, C., Omar, A.M., Ono, T., Peregon, A., Pierrot, D., Poulter, B., Rehder, G., Resplandy, L., Robertson, E., Rodenbeck, C., Seferian, R., Schwinger, J., Smith, N., Tans, P.P., Tian, H., Tilbrook, B., Tubiello, F.N., van der Werf, G.R., Wiltshire, A.J., Zaehle, S.: Global Carbon Budget 2019, Earth System Science Data, 11, 4, 1783-1838, https://doi.org/10.5194/essd-11-1783-2019, 2019.

Hoesly, R.M., Smith, S.J., Feng, L., Klimont, Z., Janssens-Maenhout, G., Pitkanen, T., Seibert, J.J., Vu, L., Andres, R.J., Bolt, R.M., Bond, T.C., Dawidowski, L., Kholod, N., Kurokawa, J.I., Li, M., Liu, L., Lu, Z., Moura, M.C.P., O'Rourke, P.R., Zhang, Q.: Historical (1750-2014) anthropogenic emissions of reactive gases and aerosols from the Community Emissions Data System (CEDS), Geosci. Model Dev., 11, 369-408, https://doi.org/10.5194/gmd-11-369-2018, 2018.

IPCC: 2006 IPCC Guidelines for National Greenhouse Gas Inventories. Eggleston, S., Buendia, L., Miwa, K., Ngara, T., and Tanabe, K. (eds.). IPCC-TSU NGGIP, IGES, Hayama, Japan. www.ipcc-nggip.iges.or.jp/public/2006gl/index.html, 2006.

IPCC: 2019 Refinement to the 2006 IPCC Guidelines for National Greenhouse Gas Inventories. Calvo Buendia, E., Guendehou, S., Limmeechokchai, B., Pipatti, R., Rojas, Y., Sturgiss, R., Tanabe, K., Wirth, T., Romano, D., Witi, J., Garg, A., Weitz, M.M., Bofeng, C., Ottinger, D.A., Dong, H., MacDonald, J.D., Ogle, S.M., Theoto Rocha, M., Sanz Sanchez, M.J., Bartram, D.M., and Towprayoon, S. (aut.); Gomez, D. and Irving, W. (eds.), Vol1. Ch.8, May 2019.

Janssens-Maenhout, G., Crippa, M., Guizzardi, D., Muntean, M., Schaaf, E., Dentener, F., Bergamaschi, P., Pagliari, V., Olivier, J. G. J., Peters, J. A. H. W., van Aardenne, J. A., Monni, S., Doering, U., Petrescu, A. M. R., Solazzo, E., and Oreggioni, G. D.: EDGAR v4.3.2 Global Atlas of the three major greenhouse gas emissions for the period 1970–2012, Earth Syst. Sci. Data, 11, 959-1002, https://doi.org/10.5194/essd-11-959-2019, 2019.

Janssens-Maenhout, G., Pinty, B., Dowell, M., Zunker, H., Andersson, E., Balsamo, G., Bézy, J.-L., Brunhes, T., Bösch, H., Bojkov, B., Brunner, D., Buchwitz, M., Crisp, D., Ciais, P., Counet, P., Dee, D., Denier van der Gon, H., Dolman, H., Drinkwater, M., Dubovik, O., Engelen, R., Fehr, T., Fernandez, V., Heimann, M., Holmlund, K., Houseling, S., Husband, R., Juvyns, O., Kentarchos, A.,. Landgraf, J., Lang, R., Löscher, A., Marshall, J., Meijer, Y., Nakajima, M., Palmer, P., Peylin, P., Rayner, P., Scholze, M., Sierk, B., and Veefkind, P.: Towards an operational anthropogenic CO_2 emissions monitoring and verification support capacity, Bull. Amer. Meteor. Soc., 0, https://doi.org/10.1175/BAMS-D-19-0017.1, 2020.

Jones, M. W., Andrew, R. M., Peters, G. P., Janssens-Maenhout, G., De-Gol, A. J., Ciais, P., Patra, P. K., Chevallier, F., and Le Quéré, C.: Gridded fossil CO_2 emissions and related O_2 combustion consistent with national inventories 1959-2018, Sci Data 8, 2, https://doi.org/10.1038/s41597-020-00779-6, 2021.

Kuenen, J.J.P., Visschedijk, A.J.H., Jozwicka, M., and Denier van der Gon, H.A.C.: TNO-MACC_II emission inventory; a multi-year (2003–2009) consistent high-resolution European emission inventory for air quality modelling, Atmos. Chem. Phys., 14, 10963-10976, https://doi.org/10.5194/acp-14-10963-2014, 2014.

Liu, Z., Guan, D., Wei, W., Davis, S.J., Ciais, P., Bai, J., Peng, S., Zhang, Q., Hubacek, K., Marland, G., Andres, R.J., Crawford-Brown, D., Lin, J., Zhao, H., Hong, C., Boden, T.A., Feng, K., Peters, G.P., Xi, F., Liu, J., Li, Y., Zhao, Y., Zeng, N., and He, K.: Reduced carbon emission estimates from fossil fuel combustion and cement production in China, Nature, 524, 7565, 335-338, https://doi.org/10.1038/nature14677, 2015.

Leutbecher, M.: Ensemble size: How suboptimal is less than infinity?, Q.J.R. Meteorol. Soc., 145 (Suppl. 1), 107-128, https://doi.org/10.1002/qj.3387, 2019.

Marland, G., Pielke Sr., R., Apps, M., Avissar, R., Betts, R., Davis, K., Frumhoff, P., Jackson, S., Joyce, L., Kauppi, P., Katzenberger, J., Macdicken, K., Neilson, R., Niles, J., Niyogi, D., Norby, R., Pena, N., Sampson, N., and Xue, Y.: The climatic impacts of land surface change and carbon management, and the implications for climate-change mitigation policy, Climate Policy, 3, 149-157, https://doi.org/10.3763/cpol.2003.0318, 2003.

Marland, G., Boden, T. A., and Andres, R. J.: Global, regional, and national fossil fuel CO2 emissions, in Trends: A Compendium of Data on Global Change, US Department of Energy, Carbon Dioxide Information Analysis Center, Oak Ridge National Laboratory, Oak Ridge, Tennessee, USA, 2006.

McNorton, J., Bousserez, N., Agusti-Panareda, A., Balsamo, G., Choulga, M., Dawson, A., Engelen, R., Kiping, Z., and Lang, S.: Representing Model Uncertainty for Global Atmospheric CO_2 Flux Inversions Using ECMWF-IFS-46R1, Geoscientific Model Development Discussions, 2020, 1-30, https://doi.org/10.5194/gmd-2019-314, 2020.

Oda, T. and Maksyutov, S.: A very high-resolution (1 km × 1 km) global fossil fuel CO_2 emission inventory derived using a point source database and satellite observations of night-time lights, Atmospheric Chemistry and Physics, 11, https://doi.org/10.5194/acp-11-543-2011, 2011.

Oda, T., Maksyutov, S., and Andres, R. J.: The Open-source Data Inventory for Anthropogenic CO_2, version 2016 (ODIAC2016): a global monthly fossil fuel CO_2 gridded emissions data product for tracer transport simulations and surface flux inversions, Earth Syst. Sci. Data, 10, 87-107, https://doi.org/10.5194/essd-10-87-2018, 2018.

Oda, T., Bun, R., Kinakh, V., Topylko, P., Halushchak, M., Marland, G., Lauvaux, T., Jonas, M., Maksyutov, S., Nahorski, Z., Lesiv, M., Danylo, O., and Horabik-Pyzel, J.: Errors and uncertainties in a gridded carbon dioxide emissions inventory. Mitigation and Adaptation Strategies for Global Change, Vol. 24, 6, 1007-1050, doi:10.1007/s11027-019-09877-2, 2019.

ODIAC: ODIAC Fossil Fuel CO_2 Emissions Dataset, available at: http://www.nies.go.jp/doi/10.17595/20170411.001-e.html, last access: 29 June 2021.

Olivier, J.G.J. and Janssens-Maenhout, G.: CO_2 Emissions from Fuel Combustion - 2016 Edition, IEA CO_2 report 2016, Part III, Greenhouse-Gas Emissions, ISBN 978-92-64-25856-3, 2016a.

Olivier, J.G.J., Janssens-Maenhout, G., Muntean, M., and Peters, J.A.H.W: Trends in global CO_2 emissions: 2016 report, JRC 103425, https://edgar.jrc.ec.europa.eu/news_docs/jrc-2016-trends-in-global-co2-emissions-2016-report-103425.pdf, 2016b.

Petrescu, A. M. R., Peters, G. P., Janssens-Maenhout, G., Ciais, P., Tubiello, F. N., Grassi, G., Nabuurs, G.-J., Leip, A., Carmona-Garcia, G., Winiwarter, W., Höglund-Isaksson, L., Günther, D., Solazzo, E., Kiesow, A., Bastos, A., Pongratz, J., Nabel, J. E. M. S., Conchedda, G., Pilli, R., Andrew, R. M., Schelhaas, M.-J., and Dolman, A. J.: European anthropogenic AFOLU greenhouse gas emissions: a review and benchmark data, ESSD, 12, 2, pp. 961-1001, https://doi.org/10.5194/essd-12-961-2020, 2020.

Pinty, B., Janssens-Maenhout, G., Dowell, M., Zunker, H., Brunhes, T., Ciais, P., Dee, D., Denier van der Gon, H., Dolman, H., Drinkwater, M., Engelen, R., Heimann, M., Holmlund, K., Husband, R., Kentarchos, A., Meijer, Y., Palmer, P., Scholze, M.: An operational anthropogenic CO_2 emissions monitoring & verification support capacity - Baseline requirements, Model components and functional architecture, European Commission Joint Research Centre, EUR 28736 EN, https://doi.org/10.2760/39384, 2017.

Super, I., Dellaert, S.N.C., Visschedijk, A.J.H., and Denier van der Gon, H.A.C.: Uncertainty analysis of a European high-resolution emission inventory of CO_2 and CO to support inverse modelling and network design, Atmospheric Chemistry and Physics, 20, 3, 1795-1816, https://doi.org/10.5194/acp-20-1795-2020, 2020.

Wang, R., Tao, S., Ciais, P., Shen, H.Z., Huang, Y., Chen, H., Shen, G.F., Wang, B., Li, W., Zhang, Y.Y., Lu, Y., Zhu, D., Chen, Y.C., Liu, X.P., Wang, W.T., Wang, X.L., Liu, W.X., Li, B.G., and Piao, S.L.: High-resolution mapping of combustion processes and implications for CO_2 emissions, Atmos. Chem. Phys., 13, 5189-5203, https://doi.org/10.5194/acp-13-5189-2013, 2013.